URBAN EXPANSION AND URBAN ENVIRONMENTAL EVALUATION IN CHENGDU, CHINA

By

Shiqi Tao

A THESIS

Submitted to
Michigan State University
in partial fulfillment of the requirements
for the degree of

Geography – Master of Science

2019

ABSTRACT

URBAN EXPANSION AND URBAN ENVIRONMENTAL EVALUATION IN CHENGDU, CHINA

By

Shiqi Tao

Environmental consequences resulting from urbanization jeopardize the life quality and social welfare of urban residents. To date, studies have focused on the urban environment by using integrated assessment methods and providing one evaluation result for the whole geographic area within an administrative boundary. These studies lack consideration of spatial heterogeneity, failing to fully understand the urban environmental statuses and dynamics at the pixel scale. Therefore, this research aims to fill this gap by systematically evaluating the urban environment at every single spatial unit of urban land against the background of urban expansion in Chengdu, a megacity in western China. Guided by a proposed three-dimensional (self, neighborhood and accessibility) theoretical framework, this study uses remote sensing and GIS data and adapts the catastrophe theory to evaluate Chengdu's urban environment in a spatially explicit manner. Results from change detection of the urban area in Chengdu show a high-speed expansion from the urban center towards all directions, especially southwest during 2000-2015. Environmental assessment analysis reveals an improved urban center but degraded outskirts regarding environmental conditions. The regression analysis suggests a negative effect of rapid urban expansion on the environment, while this effect can be alleviated through better planning strategies. Therefore, it is suggested that policy makers should balance the speed of urban expansion and urban environmental planning to provide a better living environment for urban residents in Chengdu. The integration of remote sensing and urban environmental assessment can be applied to other cities in China and elsewhere around the world.

ACKNOWLEDGEMENTS

The road is not always flat and straight, but it is full of harvest and joy. During my time at MSU, I received help intellectually and emotionally from my committees, professors, family, and friends. I am indebted to people who helped me when I came across obstacles.

I express my special thanks to my advisor Dr. Jiaguo Qi, who guides me through the way of doing research with his intellect and patience. I cannot finish the master program and be improved without his supervision. I am also eternally grateful to my committee members, Drs. Steven Pueppke, Peilei Fan, and Kyla Dahlin. I benefit so much from Dr. Pueppke for his keen intellect and meticulous attention. I offer great thanks to Dr. Fan and Dr. Dahlin who provide me with many great ideas and suggestions on research, especially this thesis work. I would also like to thank Drs. Guiying Li, Dengsheng Lu, Lifeng Luo, Geoffrey Henebry, and other faculty and staff members in CGCEO and Geography Department, for their help, advice and consideration for my research and life.

I owe exclusive thanks to my parents and grandparents for their support and encouragement. They have been offering endless love and help to me since I was born and will last forever. Many thanks to my friends and group members, Rong Zhang, Rui Zhang, Yachen Xie, Yingyue Liu, Yuhao Wang, Leah Mungai, Mimi Gong, Luwen Wan, Wei Liu, Dongyuan Wu, Jiang Chang, Myung Sik Cho, Zihan Lin and many fellow students in the center and department.

Last but not least, I thank my fiancé, Qi Zhang, for his constant consideration and support.

TABLE OF CONTENTS

LIST OF TABLES

LIST OF FIGURES

CHAPTER 1: INTRODUCTION

In the past century, the world has experienced intensive and extensive urban expansion under rapid population growth, economic development, and industrialization (Seto et al., 2011). During 1900-2000, the size of the worldwide population has quadrupled from 1.6 to 6.4 billion (Maddison, 2001), facilitating the process of urbanization. Meanwhile, the global economy, measured as Gross Domestic Product (GDP), has increased by over twenty-fold (Maddison, 2001; Krausmann et al., 2009) and the urban economy has contributed more than 90% of the value (UN, 2011).

The pace of urban area expansion is expected to continue and even accelerate in the developing world for the next century. Estimates suggest that urban land cover will increase by 1.5 million km^2, which is 2.5 times of the increased size during 1970-2000, while the urban population will increase by more than 66% by 2050 (UN, 2014) and move towards 100% by 2100 (Batty, 2011). Such huge global processes have far-reaching consequences to the terrestrial environment on the Earth as well as human well-being, particularly in developing countries. For example, urban expansion is inevitably accompanied by the tremendous demand for natural resources, such as food, water, energy, and land space for supporting residents. By 2050, almost 50% more food and biofuel, compared to those in 2012, will be needed to sustain the projected living population of 9.73 billion (FAO, 2017). Therefore, it is imperative to address the needs of sustainable development with regard to the expansion of urban areas.

There is perhaps no country where the challenge of urban sustainability is exemplified more strongly than China, currently the most populous country in the world. Since the central government implemented the opening-up policy in the late 1970s, China has witnessed a booming economy with double-digit growth in GDP over three decades (Zhang et al., 2018). Such an unprecedented increase in the economy, accompanied by the growing population, has catalyzed urban transformation and industrialization, starting from coastal cities (e.g., Shanghai, Guangzhou, Tianjin, etc.) to other major cities in the inland regions (Long, 2014). Although predominantly agrarian in history, China has become more urbanized than ever before, with urban population exceeding 55% of the total (Wu et al., 2014).

However, the fast speed of development comes with sacrifices. China has been facing numerous environmental problems such as air pollution, water shortages, sandstorms, frequent floods and droughts, as well as social issues such as inequalities (Huang et al., 2016), which have to a large extent compromised the life quality of urban residents. Thus, the main challenge is to harmonize urbanization and environmental change under the rapid pace of economic development. To address this challenge, it is necessary to conduct a comprehensive evaluation of urban expansion and environmental sustainability along with the processes.

In 2000, China initiated the western development policy, also known as the “Go West” strategic program. The goal of the policy is to reduce the growing regional disparities between the western and eastern areas, the latter being the primarily focused areas of urbanization prior to 2000. The “Go West” program aimed to promote socio-economic development in western inland areas (Lai, 2002) via investments and incentives to attract emigrants from other regions. The program covers six provinces (Sichuan, Guizhou, Yunnan, Shanxi, Gansu, and Qinghai), one municipality (Chongqing), and five autonomous regions (Tibet, Ningxia, Xinjiang, Inner Mongolia, and Guangxi), promoting economic development in western cities (Schneider et al., 2005). Although the central government included ecological conservation policies in the western development program, urban expansion has inevitably encroached onto surrounding ecosystems (e.g., farmland, wetland and forest land) and reduced ecosystem services (e.g., provisional services of food and water), jeopardizing their long-term sustainability (Liu et al., 2005). There is evidence that serious environmental issues arise because of urban expansion, including water and air pollution, loss of arable lands and reduction of biodiversity in these cities (Brown et al., 2010; Tao et al., 2013).

As the capital city of Sichuan Province, Chengdu is among the highlighted cities in western China under the “Go West” program. With fast development, the GDP of Chengdu ranks among the top two over all other western Chinese cities during the past decade. The flourishing economy has brought residents a wealthy life, but has also caused various environmental issues, threatening the life quality of urban residents. The dense construction of impervious surface intensified the effect of the urban heat island (UHI) on the city as well as its peripheral land (Zhou et al., 2014). The burning of fossil fuel led to spikes of air pollution, especially by particulate matter with a diameter less than 2.5 micrometers, namely $PM_{2.5}$ (Han et al., 2014). The growing population increased the demand for urban resources such as housing, education and green infrastructure (Schneider et al., 2005). Therefore, it is urgent to systematically evaluate the urban environment under the rapid urbanization background in Chengdu to provide suggestions to the government for better urban planning.

The present study thus aims to examine the spatial and temporal patterns of urban expansion and the urban environmental condition in Chengdu as an indirect way to evaluate the effect of economic development and issues brought about following the “Go West” program. This study has three specific aims: 1) analyzing spatiotemporal patterns and rates of Chengdu’s urban expansion during 2000-2015 with a time series of satellite observations; 2) assessing the urban environment during the study period based on a set of indicators from a spatially-explicit perspective, and 3) linking urban expansion with urban environmental conditions and discussing the effects of governmental policies. The results will provide a valuable reference to inform policy makers for the establishment or amendment of future policies for sustainable urban development in Chengdu. The linking of urban area detection and environmental assessment not only gives a spatial perspective of the urban environment but also advances the understanding of the relationship between urban expansion and urban environmental change. The proposed analysis can be applied to other urban areas in China and elsewhere in the world.

CHAPTER 2: LITERATURE REVIEW

2.1 Urbanization and urban expansion

For centuries, human activities have driven the process of urbanization on the terrestrial surface. Schwirian & Preh (1962) explained urbanization from three perspectives, including the expansion of urban area, the change of human behavior and thoughts, and the increase in urban population. Antrop (2000) defined urbanization as the process of the transformation from natural landscape to industrial types constrained by local geography and facilitated by transportation systems. Huang (2006) identified urbanization as the industrial, commercial and residential development with land cover drastically changing from natural elements to anthropogenic, rough, and rigid structures. Researchers in different fields have different views about urbanization, while all theories of urbanization are related to the changes of scopes in human and environment dimensions.

Urban expansion is an important manifestation of urbanization as a result of human needs and has pronounced consequence on the environment (Wei & Ye, 2014). Urban expansion is a process instead of status, thus requiring the track of changes over time. Many researchers reviewed reports and summarized the urban expansion processes. For example, Bengston et al., (2005) collected public discussions from news media and analyzed the consequence of urban expansion to forests in the United States. Quantifying the urban area, as most researchers propose, is a more direct way of monitoring urban expansion. Some studies used historical statistics data provided by governments about the constructed area to analyze urban expansion (e.g., Gao et al., 2014; Wei et al., 2017). However, these conventional methods were subject to errors due probably to inconsistent surveying and data processing steps by different people and the change of administrative boundaries.

With the advent and free accessibility of remotely sensed satellite images (Woodcock et al., 2008), monitoring immediate, accurate and long-term changes of urban areas within a large geographic boundary has become possible. Urban area delineation using visual interpretation methods relying on expert experiences was adopted in most of the early studies (e.g., Yagoub 2004; Henríquez et al., 2006). Liu et al. (2005) visually delineated the urban landscape and analyzed the driving forces of urban expansion in China and found an increase of 817,000 hectares in urban areas from 1990 to 2000. At the same time, indices such as the Normalized Difference Built-up Index (NDBI) were used to differentiate urban land use from other land cover types (Zha et al., 2003). A more accurate method of urban monitoring, as applied by many researchers (e.g., Chen & Masser 2003, Deng et al., 2008, Schneider & Woodcock 2008, Taubenböck et al., 2012), is to develop classification algorithms to extract urban pixels or urban objects from satellite images. Aiming to pinpoint the time of changes, Zhu &Woodcock (2014) designed an algorithm to continuously detect land use and land cover (LULC) with all available remotely sensed images, which became a popular way of tracking LULC dynamics. Inspired by previous research, Liu et al. (2019) integrated spatial-temporal rules and dense Landsat time series stack to track impervious cover in Nanchang (China) during 2000-2015. Other data, such as nightlight data derived from satellite products can also be used to reflect urban density (e.g., Henderson et al., 2003; Li et al., 2017). In addition, by using remotely sensed land surface temperature, urban land use change can influence the dynamics of UHI (Chen et al., 2006), which can, in turn, be used to facilitate the detection of urban area (He et al., 2014).

2.2 Urban environment assessment

Sustainable development, with the purpose of supporting lives for the current generation on the Earth without sacrificing benefits of the future generations, has drawn increasing attention of urban planners and the public. With the rapid urbanization process, how to sustain the living of urban residents becomes one of the most urgent topics. Focusing on social, economic and environmental dimensions, also known as the three-pillar theory, urban sustainability has been intensively studied (May, 2000; Gibson, 2006; Wang et al., 2012). Concerning sustainable urban development, many organizations, such as the United Nations, UN Human Settlements Programme, and the World Bank, have established indicator systems for evaluating urban development (Yigitcanlar and Dizdaroglu, 2015). The applications of the Urban Sustainability Indicators List (IUSIL), the Global City Indicators Facility (GCIF), and the Global Urban Indicators Database to a large variety of cities provide useful guidance for urban development (Shen et al., 2011; Fox, 2013). With the recent establishment of the UN Sustainable Development Goals (SDGs), the frontier of sustainable development embodies a broad scale of aspects considering food, water, life, climate, health, equality, etc. (Simon et al., 2016; Liu et al., 2018). One primary focus of the SDGs is building sustainable cities and communities, and the urban environment is important.

As one of the pillars of sustainable urban development, the urban environment is critical for the quality of urban residents' lives and human health (Krämer et al., 2000; Volth, 2004; Dye, 2008; Frumkin, 2016). During the past decades, the ecosystem has suffered the most from economic development in China. At the same time, the degraded urban environment, in turn, offsets economic and social development (Pacione, 2003; Nwaka, 2005). To better understand the changes, causes and consequences of urbanization, many researchers attempted to track the dynamics of the urban environment with multiple methods such as life cycle analysis (Lundin et al., 2002), system dynamic modeling (He et al., 2006), multi-agent system (Courdier et al., 2002), and linear programming (Hengsdijk & Van Ittersum, 2003). A more efficient and comprehensive approach to evaluate the urban system is using a set of relevant indicators. With each individual indicator evaluated, an integrating approach, which requires a sophisticated model (Shibata et al., 2004; Li et al., 2009; Shen et al., 2011), can be applied to all of the indicators. The result of the integration depicts a broad picture of the overall environmental condition of a city.

CHAPTER 3: METHODS

3.1 Study area

The Chengdu metropolitan area (102°54’ E - 104°53’ E and 30°05’ N - 31°26’ N) is located in the middle of Sichuan Province in western China (Figure 3.1). The central part of Chengdu constitutes the major developed area, surrounded by rural counties in the immediate vicinity of the Qionglai Mountain Piedmont to the west, and of the Longquan Mountain to the east. Two main rivers flow through the central urban area of Chengdu, providing water resources for agricultural irrigation and urban dwellings.

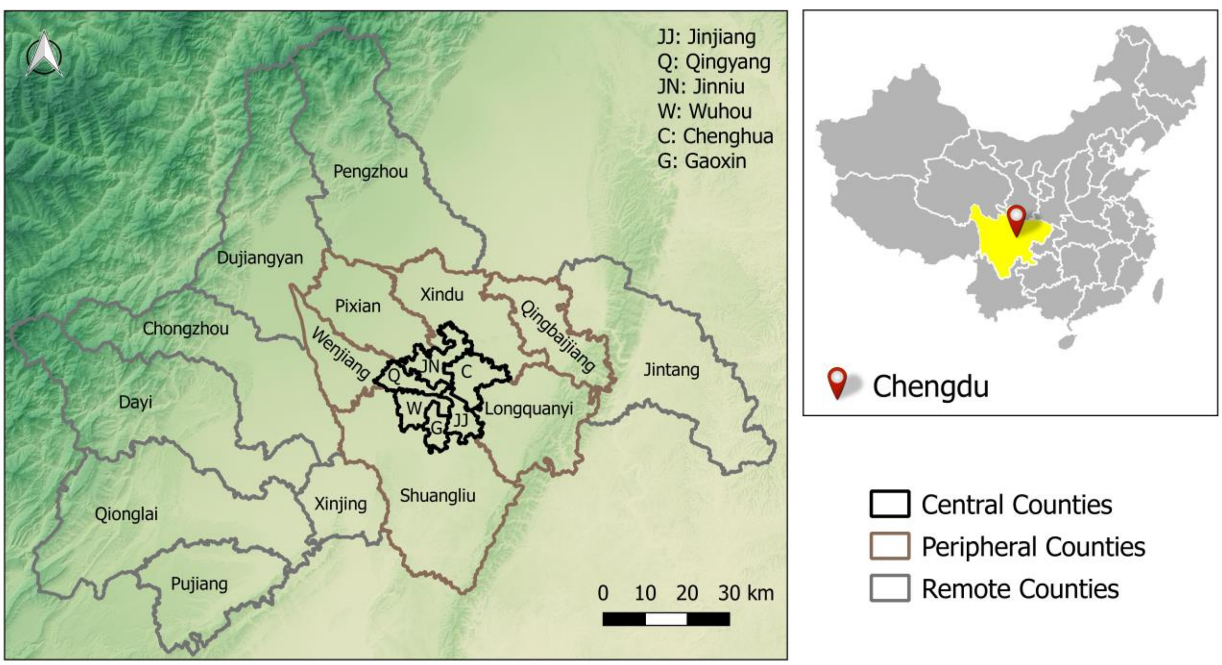

Figure 3.1. The geographic location of the study area, Chengdu, Sichuan Province in western China. The background image is topography, with darker greens representing higher elevations while light greens lower elevations.

As the capital of Sichuan Province, Chengdu is home to 14.66 million people (in 2015) within the administrative boundary, distributed over an area of 14,605 km^2, covering eleven administrative districts, five counties, and four county-level cities. The eleven districts are concentrated in the center of Chengdu, with six forming the core urban areas, while the other five are located in peripheral urban areas (Figure 3.1). Most of the counties or county-level cities in Chengdu are located in relatively remote areas dominated by natural landscapes and thus considered as suburban or rural areas. To simplify the illustration in this study, district, county and counties-level city are all called county hereafter.

Since the implementation of the "Go West" program, Chengdu has been supported by both the central and local governments for its urban development. From 2000 to 2008, Chengdu's economy witnessed a nearly threefold growth in total GDP, making the city top two in economic development among all of the western cities in China (Walcott, 2007). According to official statistics, the gross regional product of Chengdu during 2001-2015 increased from 149 billion yuan to 1080 billion yuan (~$24 billion to ~$174 billion), with per capita GDP of over 74,000 yuan (~$12,000) in 2015, which was 50% higher than the national average of 50,000 yuan (~$8,000). The total investment in fixed assets such as real estate increased by nearly 10 times during the period. Furthermore, the State Council of China designated three High-Tech Zones in Chengdu, aiming to shift the economy from agriculture, forestry, aquaculture, graziery to manufacturing (Schneider et al., 2005). Meanwhile, the local government increased investment in public transportation and infrastructures, and built ecotourism areas to provide green space amenities.

Chengdu's economic growth has caused environmental and social problems, undermining economic benefits. First, population growth, much of it driven by the arrival of rural migrants in the city, caused land shortage and traffic congestion (Hou et al., 2016). Second, urban expansion encroached onto farmlands in peripheral areas (Schneider, 2012), reducing the provision of ecosystem goods and services such as crops and livestock production. Third, the subsequent increases in energy consumption and fossil fuel burning led to air pollution. During 2009-2010, for instance, the annual average of $PM_{2.5}$ concentration in Chengdu was 165.1 ± 85.1 μg m^{-3}, far exceeding the Chinese National Ambient Air Quality Standards of 35 μg m^{-3} (below which the air quality is healthy), and the highest concentration reached as high as 425.0 μg/m^3 (Tao et al., 2013). Moreover, the high density of industrial build-ups placed Chengdu in the hazard of urban heat stresses, as observed from the remotely sensed thermal infrared data (Xu et al., 2007). Given the background of rapid urbanization in Chengdu, understanding the relationship between economic development, rapid urban expansion, environmental degradation and change in social benefits before putting adequate and effective policies into practice for sustainable development is urgently needed. Therefore, this study tracks the process of urban expansion and measures the changes in its environmental condition in an integrated way.

3.2 Data acquisition and preprocessing

Two types of spatial data were used in this study. One is remotely sensed raster data, including surface reflectance images, Digital Elevation Model (DEM), water surfaces product, land surface temperature product, and PM 2.5 data. The other is vector data, including the boundaries of all counties in Chengdu, footprints of parks, roads and rivers.

All available satellite images used in this study, including Landsat 5 Thematic Mapper (TM), Landsat 7 Enhanced Thematic Mapper Plus (ETM+) and Landsat 8 Operational Land Imager (OLI) within the study area and during the study period, were provided by the United States Geological Survey (USGS). DEM data were from the Shuttle Radar Topography Mission (SRTM). Global Surface Water Data, which has the information about the frequency of water occurrence within each pixel, was provided by the Joint Research Centre (JRC) of the European Commission (Pekel et al 2016). Daily Land Surface Temperature (LST) products from Moderate Resolution Imaging Spectroradiometer (MODIS) were obtained for creating 30 meters high-resolution Landsat-like LST data. $PM_{2.5}$ data were obtained from the Socioeconomic Data and Application Center (SEDAC) of NASA (Donkelaar et al., 2018), which can be found on the website (http://sedac.ciesin.columbia.edu). All the above-mentioned data, except $PM_{2.5}$, were obtained via the Google Earth Engine (GEE) platform (Gorelick et al., 2017).

The administrative boundary of Chengdu was obtained from the Geospatial Data Cloud (https://www.gscloud.cn). The footprints of parks, roads and river system in Chengdu were derived from Baidu Map (https://map.baidu.com/).

3.3 Extraction of urban areas

Remote sensing is a versatile technique that can capture information of the Earth's surface without direct physical contact (Lillesand et al., 2014). The advantage of remotely sensed data is that it consistently obtains timely and high-resolution information at the regional scale (Congalton et al., 2014), and hence offers more accurate and comprehensive results than traditional methods (Ouyang et al., 2016).

To generate the corresponding LULC maps, Landsat time-series images from four time periods, i.e., 1999-2001, 2004-2006, 2009-2011 and 2014-2016, were composited to a set of fully covered images representing 2000, 2005, 2010 and 2015, respectively. In the first step, cloud-free land and water pixels in all available images were identified by masking out cloud and snow pixels using the quality control information in the surface reflectance data product. Then, monthly median Normalized Difference Vegetation Index (NDVI) composites were applied to the images that are in the same month of all three years for the four-time periods. This resulted in 4 groups of 12 monthly composited images, so that within one group, each image represents each month of that year. For each year of interest (2000, 2005 2010, 2015), the maximum NDVI composition was further applied to the grouped 12 images. In this way, four fully covered composited surface reflectance images representing the years of 2000, 2005, 2010 and 2015 were created.

The Random Forest classifier (Breiman 2001; Pal 2005; Zhang et al. 2016) was employed for LULC classification. Four types of the land cover of primary interest in this research were identified, including urban, water, vegetation and bare land. A disproportionate stratified sampling scheme (Rosenfield et al., 1982; Congalton 1991) was adopted to select pixels for training the classifier. Since urban land consists of the most complex surface characteristics and vegetation covers most of the study area, more than 100 locations comprised of over 1500 pixels in these two classes each were selected as training samples. In addition, more than 500 pixels of water, more than 1200 pixels of bare land were used for training. The major error of classification exists between urban and bare land that have similar spectral information. Thus, topographic and geographic information including slope and distance to water was used to distinguish between these two classes (Zhang et al., 2018), given that bare land is mostly located in proximity to rivers while the urban land cover is flat in Chengdu. Therefore, slope derived from DEM data, and distance to water calculated based on water occurrence data were then overlaid to the composited images and included as training features in the random forest algorithm. The parameter setting for machine learning algorithms is one of the key factors for classification accuracy. Following the suggestion by a previous study (Belgiu & Drăguţ, 2016) and adjusted during the process of classification, the number of decision trees to create per class was set to 500; the number of variables per split was set to the square root of the number of variables; the minimum size of a terminal node was set to 3, and the fraction of input to bag per tree was 70%. To test the accuracy of the classification results, a set of 800 testing sample points containing the four different classes were stratified sampled using the combined map of four classified LULC results. In this way, all 256 classes include 800 points are sampled. Some sample points, whose ground truth were hard to recognize mostly because of the shadow, cloud and high aerosol cover, were excluded from accuracy assessment. Therefore, the number of final testing samples is less than 800 pixels.

3.4 Derivation of environmental indices

3.4.1 Urban greenness

In this study, two indicators were used to represent greenness, which is an important criterion of favorable urban environments. The first is the NDVI, an index that has been widely used for tracking healthy vegetation with remote sensing techniques (Rouse, 1973; Bannari et al., 1995; Kawabata et al., 2001). The higher the index value, the higher the vegetation cover. The index can be derived based on the surface reflectance at the radiative wavelengths of 0.66 μm (Red Band) and 0.86 μm (Near-Infrared Band), given the knowledge that the chlorophyll in the vegetation absorbs red radiance while strongly reflects near-infrared radiance. Thus, the index can be expressed as a function of red reflectance (SR_{red}) and near-infrared reflectance (SR_{NIR}), as shown in Eq. (3.1)

$$NDVI = \frac{SR_{NIR} - SR_{red}}{SR_{NIR} + SR_{red}} \tag{3.1}$$

Because of the sensor difference between Landsat 5 TM, Landsat 7 ETM+ and Landsat 8 OLI, only Landsat 7 was used to calculate NDVI except for the year of 2015. The NDVI value was calculated for each cloud-free pixel of all the available Landsat 7 ETM+ images for 1999-2001, 2004-2006, 2009-2011, 2014-2016. For each three-year period, a maximum NDVI composite was generated to represent the annual greenness for each pixel. Because of the Landsat 7 ETM+ failure of Scan Line Corrector (SLC), the quality of the image was reduced with the occurrence of data gaps (Wulder et al., 2008). This gap effect makes the reflectance values of adjacent pixels in strip areas of the composted image inconsistent. This inconsistency needs to be alleviated by using the composition of three years' data. However, for the year of 2005, due to both high cloud cover and the strip effect, there was still a limited amount of available information for the Landsat 7 ETM+ images. To solve this problem, the Landsat 5 TM images were included for the period of 2004-2006.

The second type of data pertains to parks, a special type of greenness that provides residents a place to relax (Ulmer et al., 2016, Kondo et al., 2018). Park footprints were obtained using Baidu Map, representing the year of 2015. To trace back to the years where park information was not available, the difference of NDVI values within each park between the year of 2015 and the year of interest was calculated as a reference to determine if the park had already been built since the year of interest. The first step is to subtract the maximum NDVI image of 2015 by the year of interest (2000, 2005, 2010). Then, the Mean Square Error (MSE) within each park was calculated. Finally, a 0.06 threshold of MSE was empirically defined to exclude the parks that had not been built during the previous years. This park counting method assumes that a park would not be removed once it was built during 2000-2015. Using the MSE of NDVI values, the information of parks on the four years were obtained. Figure 3.2 illustrates the distribution of MSE between 2015 and the years of interest with the empirically defined threshold to exclude parks.

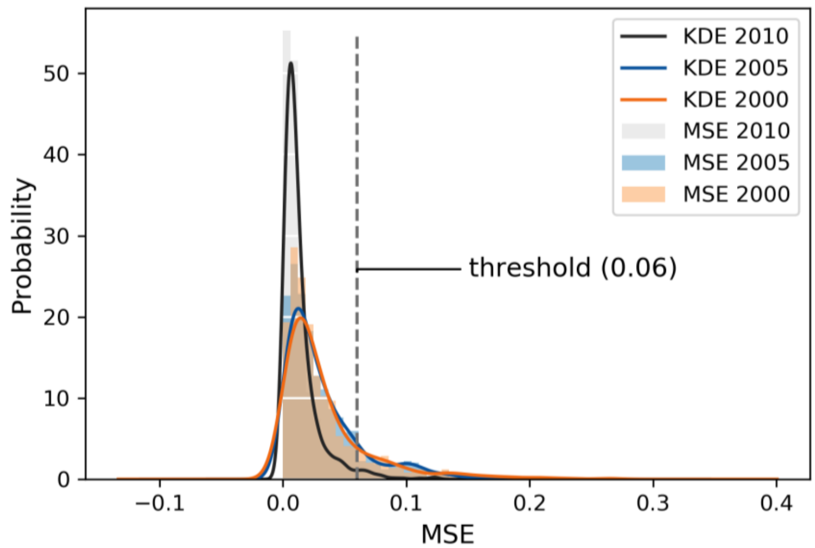

Figure 3.2. Histograms of MSE (NDVI difference between 2015 and 2000/2005/2010 within parks) and smoothed distribution using the kernel density estimation. The area of each column in each histogram equals to the probability of data distribution at that range. The threshold was empirically set as 0.06 to determine whether the park was already built at that time.

3.4.2 Urban blueness

The blueness in urban is defined as large open water (Gascon et al., 2015, Pitt 2018) that is believed to have a beneficial function on reducing residents' psychological distress (Nutsford et al., 2016). To delineate water surfaces with relatively large areas, water pixels were extracted from the classified satellite images for each year. Next, to remove small ponds, and most importantly, the noise (classification error), the count of each water pixel cluster was calculated, and the clusters with fewer than 10 pixels (around 9000 m^2) were removed. Because many rivers in Chengdu have widths less than 30 meters, some of them cannot be distinguished from satellite images through classification. Therefore, the shapes of rivers obtained from Baidu Map were converted to raster data and combined with data of large water bodies.

The Normalized Difference Water Index (NDWI) is another indicator of urban blue. There are two commonly used NDWIs, with one indicating the water content in vegetation (Gao 1996), and the other indicating the water content in the water body (McFeeters 1996). For the purpose of this study, the index defined by McFeeters (1996) was used to calculate the water content in each pixel. With SR_{green} represents the green band and SR_{NIR} represents the NIR band of the surface reflectance image, the algorithm of the NDWI is shown as follows:

$$NDWI = \frac{SR_{green} - SR_{NIR}}{SR_{green} + SR_{NIR}} \tag{3.2}$$

3.4.3 Air quality

Air quality is considered one of the most important factors that influence the well-being of urban residents. Air pollutants such as $PM_{2.5}$, PM_{10}, NO_2, and SO_2 are all proved to have negative impacts on human health (He et al., 2001; Weinmayr et al., 2009; Pui et al., 2014). However, except for $PM_{2.5}$, there is no accessible air pollutant data with high spatial resolution suitable for the study area. At the same time, the high concentration of sulfur contents, diesel and road dust in $PM_{2.5}$ (He et al., 2001) make it an ideal indicator to analyze air pollution. Therefore, $PM_{2.5}$ data with a spatial resolution of 0.01 degree were obtained and used to derive the air quality indicator. To align the spatial resolution according to those of other spatial data, the bicubic resampling approach (Carlson & Fritsch 1985) was conducted to generate $PM_{2.5}$ data with a spatial resolution of 30 meters for the four years of interest in Chengdu. The bicubic sampling process predicts every geographic unit using an interpolant that is determined by the first partial derivatives and first mixed partial. The resampled data approximates real value at each pixel under the assumption that the concentration of $PM_{2.5}$ changes gradually in the air.

3.4.4 Land surface temperature

LST measures the temperature of the land surface within a unit area, which is a strong indicator of the urban environment (Yue et al., 2012). There are many existing methods for deriving LST, such as the mono-window algorithm (Qin et al., 2001), the single-channel algorithm (Jiménez-Muñoz et al., 2009), and the radiative transfer algorithm (Yu et al., 2012). These methods require ancillary data about atmospheric conditions, which are not available in this research. Thus, this study used the effective at-sensor brightness temperature, which is Band 6 in surface reflectance data of TM and Band 8 of OLI data, to calculate LST through a method that requires only information of the NDVI (Weng 2003; Li et al., 2009; Shen et al., 2016).

The at-sensor brightness temperature is referenced to a "black body", which should be differentiated from the properties of real objects. Therefore, the equation (Artis & Carnahan, 1982) to correct the spectral emissivity is applied, written as:

$$LST = \frac{T_{sensor}}{1 + (\lambda \times T_{sensor} \,/\, \alpha) \ln(\varepsilon)} \tag{3.3}$$

where T_{sensor} is the effective at-sensor brightness temperature in Kelvin (K); LST is the surface radiance temperature in K; λ is the wavelength of the emitted radiance in meters; α = 1.438×10^{-2} mK; ε is the surface emissivity. For water (NDVI < 0) pixels, ε were assigned a value of 0.9925; in urban (impervious surface) and bare land ($0 \le$ NDVI < 0.15), ε were assigned a value of 0.923 (Xie et al., 2012); while in highly vegetated area (NDVI > 0.727), ε were assigned a value of 0.986 (Valor & Caselles, 1996). For all the other NDVI values, the following equation (Van de Griend & Owe, 1993) was used:

$$\varepsilon = 1.0094 + 0.047 \ln(NDVI) \tag{3.4}$$

Here, the reference NDVI value was calculated using the surface reflectance data with Eq. (3.1). Using the NDVI method illustrated above, land surface temperature derived from all the available Landsat images during summer (June-August, Figure 3.3) in Chengdu was calculated. To generate a fully covered summertime LST map, a median composition was applied based on the calculated LST time series data during the summer in three-year intervals for each year of interest. In detail, for example, the median value of LST for each pixel within June-August from 1999 to 2001 was calculated to generate the map of summer median LST for the year of 2000. The process was applied in parallel to the other three years of interest, i.e., 2005, 2010, 2015.

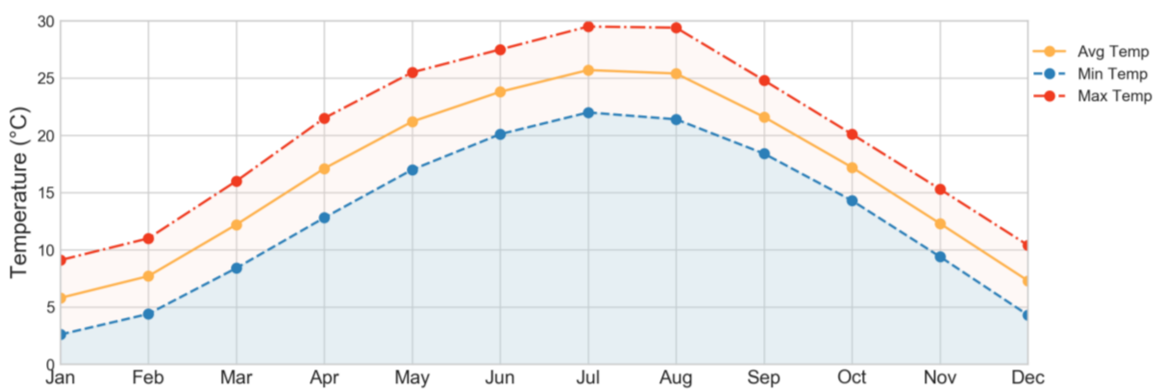

Figure 3.3. Monthly temperatures in Chengdu. The highest temperature is in the summertime, June-August. (source: https://en.climate-data.org/)

For the year 2005, however, the number of available pixels during summer was not enough to cover the whole study area due to high cloud cover. Therefore, the MODIS summer median LST in 2005 was calculated and combined with surface reflectance images of 2005 to predict the

Landsat-like LST data at the 30-meter spatial scale. First, MODIS LST data were resampled from 500 meters to 30 meters using the bicubic algorithm (Carlson & Fritsch 1985). Second, summer median LST from MODIS was combined with the composited surface reflectance data (the image previously used for classification) and used as the training bands, while Landsat LST data were used as training results on the data of 2000. A machine learning method was used to do the prediction, with stratified random samples selected including 5000 pixels for urban and vegetation classes each, and 2000 for water and bare classes each. Then, a random forest regression was applied to the sampled training set to predict the Landsat-like LST on each of the land cover classes separately. If the samples from only one specific class were used for the training, the error would be high for the misclassified pixels within that classified land cover. Therefore, this study proposed to include sample pixels from other land cover types in the training process to minimize the error. To understand the influence of the proportion of different training samples on the regression accuracy, the mean square error (MSE) between simulated and actual LST values was calculated after the prediction using different combinations of samples on different land cover. With every 5 percent increase of pixels sampled on one specific land cover (the rest of pixels are sampled on other land cover types), the MSE was plotted based on 20 simulations (training samples were spatially random at each simulation). The percentage that corresponds to the lowest MSE was then chosen to predict the LST in 2005.

3.4.5 Natural environment

The natural environment provides many mental and physical benefits to human beings (Hartig et al., 1991, Mitchell & Popham, 2008). In this study, the natural environment is defined as the area with a limited human-dominated area within a region. Therefore, the natural environment is mapped based on the criteria that the urban land cover should be less than a certain percentage of all the land covers within a certain distance. Specifically, a buffer of 1000-meter radius was delineated for each pixel of classified images, and the percentage of urban area within the buffer was calculated. Then, a 1% threshold was empirically set to distinguish natural and human-disturbed environments. The 1% threshold is appropriate for countries (e.g., China) where urban expansion is compact.

3.5 Dimensions for assessing environmental condition

3.5.1 Theoretical framework

To achieve the goal of evaluating environmental sustainability, a theoretical framework that includes different dimensions of indicators for analyzing the condition of the urban environment of Chengdu was proposed. The spatial disparity within one city suggests that a location-based evaluation (evaluating the condition within a unit of geographic area) of environmental conditions is more sophisticated than an overall evaluation (one score for one whole region) (Metzger & Schröter, 2006). Therefore, the first dimension chosen in this study is the environmental condition within an individual spatial unit. Apart from the environment of a certain location, the nearby environment also supports the social well-being of urban residents (Unger & Wandersman 1982). For example, Nuissl et al. (2002) analyzed the environmental impact of land use change and suggested to include the influence of changes in the neighboring landscape when examining spatial interrelations. Therefore, the second dimension is the neighboring environment. With the expansion of urban areas, accessibility becomes one of the most important factors in the changing landscape (Antrop 2004). This indicates that characterizing the living environment also requires the measurement of residents' access to favorable environmental infrastructures, which was calculated and chosen as the third dimension of the environmental condition proposed in this research. With all the three dimensions encompassed, the theoretical framework of the urban environment was constructed to guide this research (Figure 3.4). To have a spatially explicit evaluation of the urban environment, the indicators at every single geographic unit (i.e., a pixel of image) within the study area were evaluated in order to assess the spatial disparity of environmental condition.

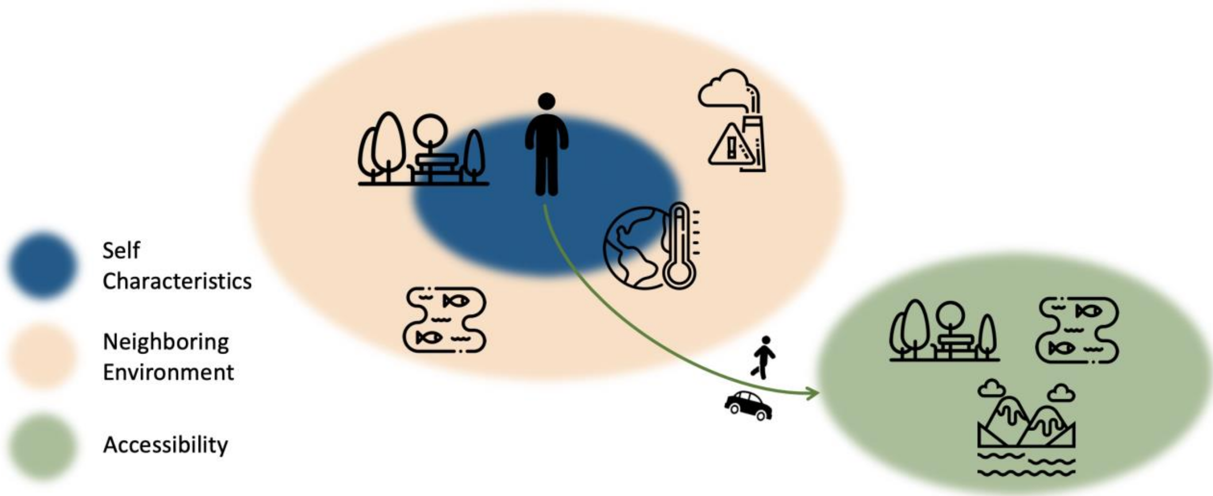

Figure 3.4. The theoretical framework of three dimensions for assessing the urban environment in Chengdu. The characteristics within the blue region represent the environmental condition in the pixel itself. The neighboring environment means the environmental condition within a certain buffered zone that is walkable to residents. The accessibility dimension is a way to measure the degree of convenience for residents to access one specific location.

Aggregating the indicators within a constructed model is as important as the evaluation of the selected indicators. Explicit grading methods such as mean aggregation, weighted aggregation and experts' grading (Krajnc et al, 2005; Van de Kerk) lack of objectivity. Other implicit methods such as principal component analysis (Li et al., 2012) and project pursuit model (Shao et al., 2015) integrate the variables depending on the data distribution, which makes these approaches data-driven with few interpretable implications. Among all the approaches of integrating urban environment indicators, the catastrophe model has received increasing attention (Clarke and Wilson, 1983; Wilson, 2011) because the model clearly describes and simulates the behavior of gradual changes, followed by an abrupt transformation that resembles most of the systems in the real world. The catastrophe theory delineates the tipping points from quantitative change to qualitative change, which contradicts the linear relationship between variables and a system. The catastrophe theory uses the implicit weighting process by changing the data distribution of indicators depending on the relative importance of indicators. For each step that requires catastrophe model weighting, a more important indicator will be less transformed so that the resulting value will be more similar to its original status. Su et al. (2011) used the catastrophe model to evaluate land ecological security in Shanghai and found a significant downward trend of land eco-security during 1999-2008. Yang et al. (2012) assessed urban water security based on catastrophe theory and compared it with other methods. The result demonstrated the reliability and scientific significance of the catastrophe theory. Zhou et al. (2018) applied the catastrophe theory in assessing eco-security of plastic greenhouse soil and suggested that this method has strong objectivity. Overall, the catastrophe theory has a unique advantage against others with its wide applicability and objectivity, which gives it promising applications in environmental evaluation based on indicator systems. Thus, this study used the catastrophe model to evaluate urban environmental condition under the guidance of the proposed three-dimension theoretical framework.

3.5.2 Self attributes

As the most important dimension of the urban environment, the unit itself has the closest contact with people who live at that location. Within each unit, the greenness, temperature and air quality directly impact the mental and physical health of residents. However, air quality data often has a coarse spatial resolution (1000 meters in this study), thus it is not representative within the spatial unit of the present study, which has a 30-meter resolution. At the same time, because there supposed to be no water within pixels which were classified as urban, indicators related to water were not used in this dimension. Therefore, two indices were derived for each pixel to represent the environment sustainability status of the pixel itself, including the NDVI and the LST. The detailed calculation steps are illustrated in sections 3.4.1 and 3.4.4.

3.5.3 Neighborhood characteristics

For each pixel, the environmental status can also be influenced by conditions in the surrounding areas, in addition to those within the pixel itself. Many researchers defined the neighborhood using a circular buffer with a radius from 400 to 1000 meters (Colabianchi et al., 2007; Root 2012), and 400 meters is the most walkable distance (Bissonnette et al., 2012). In order to adjust to the local situation, neighboring regions are defined as a 500-meter buffer zone in this study, which equals to the distance of two blocks on average in Chengdu. Local residents are expected to have most of their daily activities within two blocks of their residence. In the neighboring region, greenness, blueness, temperature and air quality all have impacts on residents' health. Therefore, four indices were calculated to measure the neighborhood environmental characteristics given a specific pixel, including NDVI, NDWI, LST and $PM_{2.5}$.

3.5.4 Accessibility

Accessibility to the public natural environment is another way of defining the urban environmental condition. In this study, three places were considered as the natural environment. The first is the park, a typical type of urban green space, which provides citizens numerous physical and mental health benefits (Lee et al., 2010, Hartig et al., 2014). The second is large open water.

Blue spaces are known to be associated with the healthy lifestyles of residents (Gascon et al., 2015), and in this study, they are defined as rivers and large open water surfaces. The third is the rural area, which has most of the natural green land cover in Chengdu and is also beneficial to urban residents. In this study, rural areas are defined as places with less than 1% of the urban land cover within a 1000-meter buffer zone. The accessibility was then calculated using the friction map (Weiss et al 2018) of Chengdu.

Two kinds of friction maps, driving friction map and walking friction map, were derived using road data obtained from Baidu Map. They were created by dividing the length of the pixel by speed. For driving speed, highways were assigned a value of 110 km/h; national and province-level roads 70 km/h; county-level roads 50 km/h; narrow roads in urban area 30 km/h; other roads 40 km/h. Pixels lacking roads were assigned a value of 5 km/h, which corresponds to walking speed. In the walking speed map, roads were given a value of 5 km/h while other pixels 4 km/h.

The friction maps allow the calculation of accessibility to parks/water represented by the time cost of each pixel to the nearest park/water via walking. Accessibility to the rural environment is defined as the time cost of each pixel to the nearest rural area via driving. For each pixel, a smaller time cost indicates better accessibility.

3.6 Catastrophe model development

3.6.1 Indicator selection and initialization

Based on the theoretical framework and urban environmental indicators illustrated above, the indicator system of urban environmental assessment using the hierarchical analysis was shown in Table 3.1, with a total of three dimensions including nine indicators.

Table 3.1. Indicators and structure of the catastrophe model applied in this study.

Dimension	**Indicator**	**Description**
Direct impact [A]	Vegetation greenness [B1]	Annual maximum NDVI
	UHI effect [B2]	Median LST in summer
Neighboring effect [A2]	Air quality [B3]	Annual mean $PM_{2.5}$ in neighboring regions
	Neighboring vegetation greenness [B4]	Spatial averaged maximum NDVI in neighboring regions
	UHI effect in the neighboring environment [B5]	Spatial averaged median LST in summer of neighboring regions
	Neighboring blue surfaces [B6]	Spatial averaged NDWI in neighboring regions
Accessibility [A3]	Access to public parks [B7]	Cumulative time cost to the nearest park
	Access to urban blue [B8]	Cumulative time cost to the nearest open water surfaces (lakes/rivers)
	Access to a rural area[B9]	Cumulative time cost to a rural area

The units and data range of the indicators are different so they are not comparable and cannot be integrated together before the transformation. To transform the data, all indicators need to be rescaled to a range between 0 and 1. Two types of formulas are used because some of the indicators (B1, B4, B6) have positive influences on the urban environment, while others (B2, B3, B5, B7, B8, B9) have negative influences. For the indicators with positive influence, a higher value means a better urban environment, so that the equation can be written as:

$$X_i = \frac{x_i - x_{min}}{x_{max} - x_{min}} \tag{3.3}$$

For the indicators that have negative influences the on the urban environment, a higher value of the data means a poorer urban environment. In this case, the equation can be written as:

$$X_i = \frac{x_{max} - x_i}{x_{max} - x_{min}} \quad (3.4)$$

3.6.2 Catastrophe model framework

Table 3.2. Illustration of different categories of catastrophe models defined by the number of control variables. (source: Woodstock and Poston, 2006)

Category	Number of control variables	Potential function	Bifurcation set	Normalization formula
Fold model	1	$V(x) = 1/3x^3 + u_1x$	$u_1 = -3x^2$	$X_{u1} = u_1^{1/2}$
Cusp model	2	$V(x) = 1/4x^4 + 1/2u_1x^2 + u_2x$	$u_1 = -6x^2$, $u_2 = 8x^3$	$X_{u1} = u_1^{1/2}$, $X_{u2} = u_2^{1/3}$
Swallowtail model	3	$V(x) = 1/5x^5 + 1/3u_1x^3 + 1/2u_2x^2 + u_3x$	$u_1 = -6x^2$, $u_2 = 8x^3$, $u_3 = -3x^4$	$X_{u1} = u_1^{1/2}$, $X_{u2} = u_2^{1/3}$, $X_{u3} = u_3^{1/4}$
Butterfly model	4	$V(x) = 1/6x^6 + 1/4u_1x^4 + 1/3u_2x^3 + 1/2u_3x^2 + u_4x$	$u_1=-10x^2$, $u_2 = 20x^3$, $u_3 = -15x^4$, $u_4 = 4x^5$	$X_{u1} = u_1^{1/2}$, $X_{u2} = u_2^{1/3}$, $X_{u3} = u_3^{1/4}$. $X_{u4} = u_4^{1/5}$

The catastrophe theory was introduced to describe abrupt changes triggered by continuous alteration of multiple influencing factors. The behavior and function that describe the system are different given different numbers of variables at each level (Su et al., 2011). The general forms of the catastrophe model were described in detail by Woodstock and Poston (2006). In this study, given the number of variables within each sub-system, the general form of the model is described in Table 3.2.

With the variables selected (Table 3.1) and the normalization formula illustrated (Table 3.2), the catastrophe models were then applied to evaluate the urban environment in Chengdu using the normalization formulas defined by the number of variables. The modeling process is shown in Figure 3.5.

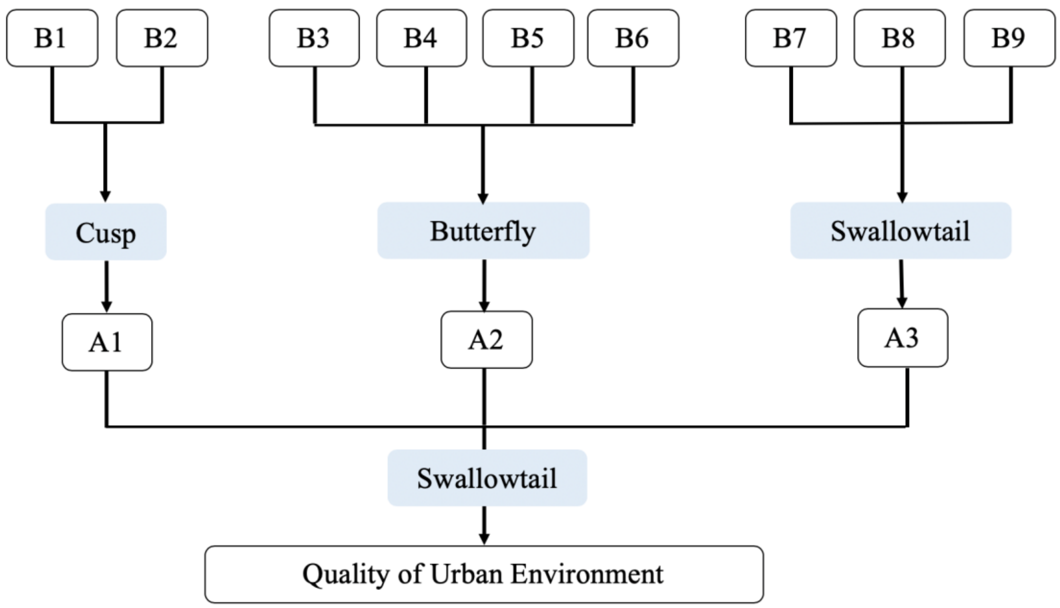

Figure 3.5. Indicator system, hierarchical model structure and selected catastrophe model for each sub-system of urban environmental evaluation.

3.7 Regression between urban expansion and urban environment

To link urban expansion and urban environment, univariate linear regression models were applied to all counties in Chengdu, i.e., county is used as the analyzing unit. As many researchers pointed out, the rapid urban expansion would bring stress to the local urban environment in China (Li et al., 2013). Therefore, an assumption is that the larger the expanded area, the less improvement (or the greater deterioration) will the urban environment changed from the previous stage (year). In this case, the null hypothesis to test is that with the increase of the expanded area, there is no influence on the change of the urban environment. To test this assumption, the expanded urban area between the adjacent two selected years was used as an independent variable, and the change of urban environmental assessment value was used as the dependent variable. In this study, three models were applied separately to each of the three time periods (2000-2005, 2005-2010, and 2010-2015) to explore the relationship between urban expansion and urban environment.

CHAPTER 4: RESULTS

4.1 Urban expansion

4.1.1 Accuracy assessment for classification

Before interpreting urban expansion results, it is necessary to show the accuracy metrics of the classifications. Using stratified sample points that were selected from the combined image of four LULC maps, the confusion matrix (Stehman 1997) for each classified image was created and shown in Tables 4.1-4.4. The total number of testing samples is nearly 800 pixels, and the same samples were used for the four images in different years. The overall testing accuracies for the images of 2000, 2005, 2010, and 2015, calculated by dividing the correctly classified pixels by the number of all testing pixels, were 83.2%, 79.6%, 84.3%, and 80.9%, respectively.

Table 4.1. Confusion matrix of random forest classification in 2000.

		Truth				
		Urban	Water	Vegetation	Bare land	Total
Classified	Urban	123	15	0	50	188
	Water	10	147	15	6	178
	Vegetation	2	10	185	0	197
	Bare land	15	2	4	185	206
	Total	150	174	204	241	769

Table 4.2. Confusion matrix of random forest classification in 2005.

		Truth				
		Urban	Water	Vegetation	Bare land	Total
Classified	Urban	140	21	5	40	206
	Water	10	149	12	5	176
	Vegetation	19	11	153	5	188
	Bare land	15	2	12	172	201
	Total	184	183	182	222	771

Table 4.3. Confusion matrix of random forest classification in 2010.

		Truth				
		Urban	Water	Vegetation	Bare land	Total
Classified	Urban	138	11	5	37	191
	Water	5	154	2	3	164
	Vegetation	5	10	176	3	194
	Bare land	31	4	1	160	196
	Total	179	179	184	203	745

Table 4.4. Confusion matrix of random forest classification in 2015.

		Truth				
		Urban	Water	Vegetation	Bare land	Total
Classified	Urban	129	14	0	41	184
	Water	12	169	10	2	193
	Vegetation	4	12	177	1	194
	Bare land	45	1	2	134	182
	Total	190	196	189	178	753

Based on the confusion matrix, producer's accuracy pertaining to the omission error and user's accuracy relating to the commission error can be derived. Producer's accuracy is calculated as the percentage of sample pixels that were correctly classified in a given class while user's accuracy is the proportion of predicted pixels in a given class that is truly in that class. Focusing on the urban land, both producer's accuracy and user's accuracy fell within a satisfactory range of 65%-82%. In 2000, the producer's accuracy was 82.0%, while the user's accuracy was 65.4%. In 2005, compared to 2000, the classification of the urban area had a greater omission error but a smaller commission error, with producer's and user's accuracies of 76.1% and 68.0%, respectively. In 2010, both producer's accuracy (77.1%) and user's accuracy (72.3%.) were higher than those in 2005, respectively. For the image of 2015, the producer's accuracy (67.9%) was the lowest among the four images, while the user's accuracy (70.1%) was in the middle of the range.

As Chengdu is at the middle state of urban development, its LULC change followed expected orders. For example, it is typical that vegetation was converted to bare land, which then changed to urban. However, it is the least likely that urban would change back to water and to bare land. Thus, the aforementioned stratified sampling process implemented in this study tended to select incorrectly classified pixels comparing to the spatially random sampling process. Therefore, the actual accuracy for the whole Chengdu city should be much higher than the reported accuracy.

4.1.2 Urban expansion area

The spatial pattern of urban expansion reveals that, between 2000 and 2015, Chengdu experienced a rapid increase in urban areas, with urban land encroaching on surrounding land cover in all directions, especially to the southwest (Figure 4.1). The majority of the expanded urban areas were located within the peripheral counties, while remote counties had much fewer and scattered areas of expansion (Figure 4.1a).

To have a detailed view of urban expansion in Chengdu, the expanded areas towards eight directions were calculated within a buffer whose radius equaled to two times of the area of the central counties (Figure 4.1b). The rates of expansion in different directions varied substantially. The spider chart (Figure 4.1c) verifies that most urban areas expanded in four directions: northwest, west, southwest and south, where all encroached areas are calculated to be more than 120 km^2 by 2015. West, which had the least urban cover in 2000, became one of the two highest urbanized regions by the year of 2015. North, northeast and southeast experienced substantial encroachment, but had relatively small urban areas, compared to the aforementioned four directions. The urban areas in these three directions all reached 90 km^2 during the 15 years. The eastern part of Chengdu had the slowest pace of urban expansion, with an urbanized area less than 90 km^2.

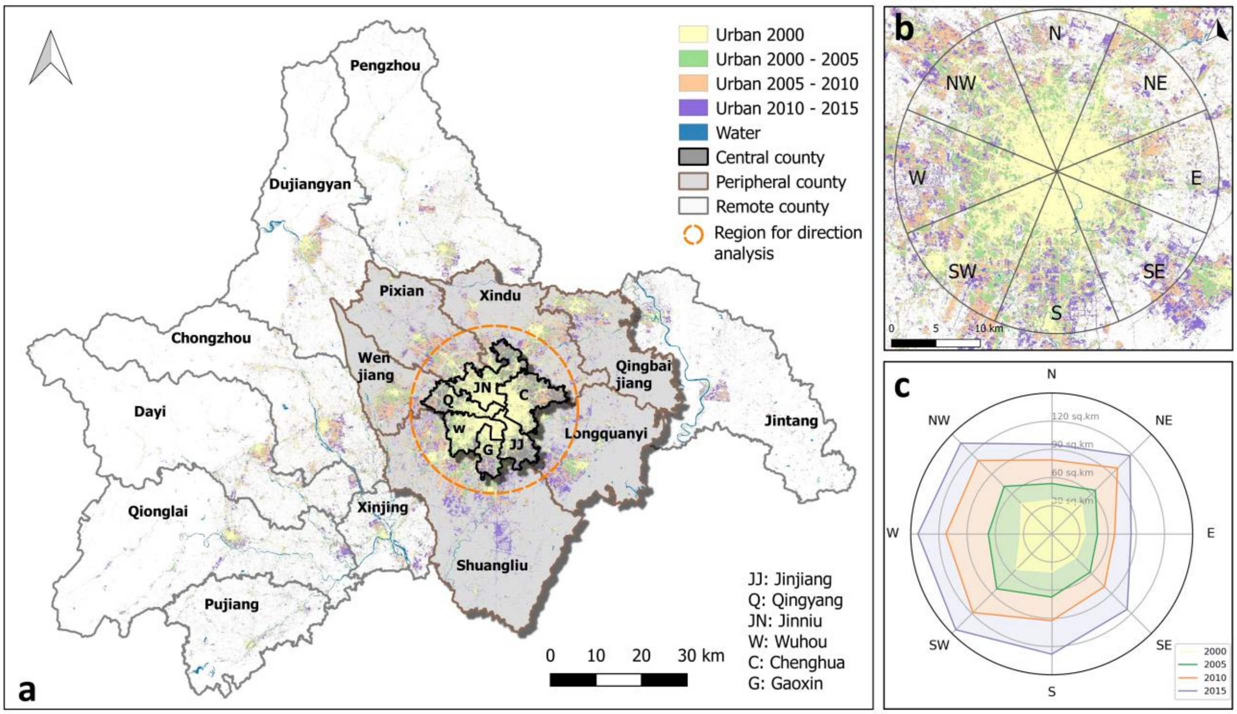

Figure 4.1. (a) Urban expansion of Chengdu showing different spatial and temporal patterns within the central, peripheral and remote counties. (b) Zoomed-in analysis of urban expansion within the circular region (bounded by the orange dash line in subplot a) that covers all central counties and some peripheral counties, with the legend the same as the one in subplot a. (c) Spider plot of urban expansion analysis within the circular region showing that the urban area in Chengdu expanded mostly towards the west and south.

Figure 4.2 provides the graphic results of urban expansion areas and rates during the study period at the county level. Overall, the urban area of Chengdu expanded to a substantial extent during 2000-2015. The urban area was concentrated within central counties in 2000, but the peripheral area has the greatest urban area in 2015. For central counties, the total urban area in 2000 was 220.6 km^2, which increased to 379.4 km^2 in 2015 with an increaseing rate of 72.0% over the 15-year study period and a mean annual increase rate of 4.8%. Among all the central counties, Jinniu had the largest urban areas in both 2000 and 2015, with the urban area in 2015 accounting for 78.6% of the total county area. Compared to the other central counties, Gaoxin had the greatest expansion rate (135.7%) during 2000-2015. The percent cover of the urban area in Gaoxin reached 90.4% in 2015, although the total district area is relatively small (only 470.3 km^2). The expansion of the central counties saturated within the bounded county region, which is the main reason that those central areas were not the most expanded area.

All counties in the peripheral region went through rapid urban expansions with increase rates of over 300%. Among all the peripheral counties, the largest expanded urban area (in square kilometers) occurred in Shuangliu, while the greatest urban expansion rate was observed in Wenjiang. In addition, the total urban area of Shuangliu also achieved the greatest amount over all the counties in the whole study area in 2015. Wenjiang had the least urban area in 2000, which however increased to 81.3 km^2 in 2015, a number larger than most counties in Chengdu.

The urban extent in remote counties was the smallest among the three regions in 2000, but all of these counties experienced tremendous urban expansion during the 15-year period. The highest rate of expansion (627.6%) was found in Jintang county, followed by Dayi (516.6%). The total urban area in remote regions in 2015 was 535.0 km^2, revealing a huge jump since 2000 (105.8 km^2). These results provide a statistical view on the spatial heterogeneity of urban expansion by the administrative boundary.

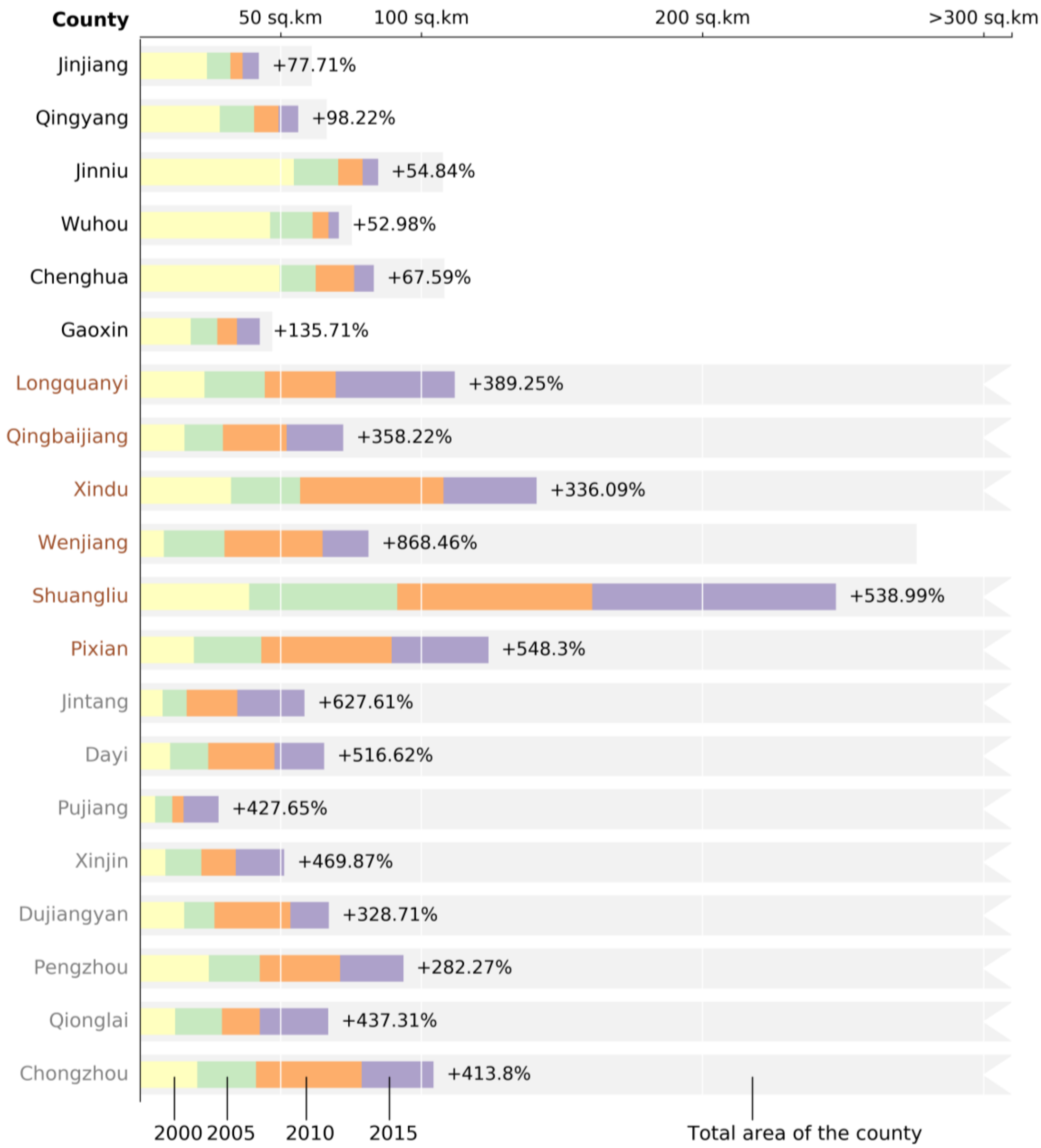

Figure 4.2. Urban expansion area and the percentage by county of Chengdu. County names in the central region are shown in black text, peripheral counties brown, and remote counties gray. Gray bars refer to the total area of a given county, while yellow bars represent urban areas in 2000, green bars show the expanded area during 2000-2005, orange bars 2005-2010, and purple bars 2010-2015.

4.2. Urban environmental indicators

4.2.1 Accuracy of simulated surface temperature data

In this study, the LST data in 2005 was derived using a machine learning algorithm, which required accuracy assessment as did the image classification. In order to avoid the data limitation due to insufficient images covering the whole study area in the summertime of 2005, a random forest approach was implemented to simulate the 30-meter LST data using MODIS LST as reference. To understand the influence of the proportion of different training samples on the accuracy, the mean square error (MSE) between simulated LST value and actual value was calculated, and the mean value and envelope of 20 simulations were plotted for every 5 percent increase of pixels in actual land cover. Figure 4.3 shows the influence of percentage change of training samples on the training accuracy. Take LST prediction on urban land as an example, there were totally 4000 training samples used, with some from the pixels in urban land cover and the rest from the other land cover types. With the increase of the percentage of urban land pixels as training samples, the MSE in the urban area decreased, while the MSE in other land cover types gradually increased and finally reached the tipping point at 95%.

To achieve high accuracy, according to the MSE charts, 95% of the urban pixels and 5% of the other pixels were combined together to train the LST random forest using the samples in 2000's image and the classifier was applied to 2005's data. Similarly, 95% of vegetation pixels and 5% of the other pixels were selected on areas covered with vegetation. For water and bare land, 80% of the pixels in the actual land cover class and 20% of the pixels in other LULC types were used as training samples.

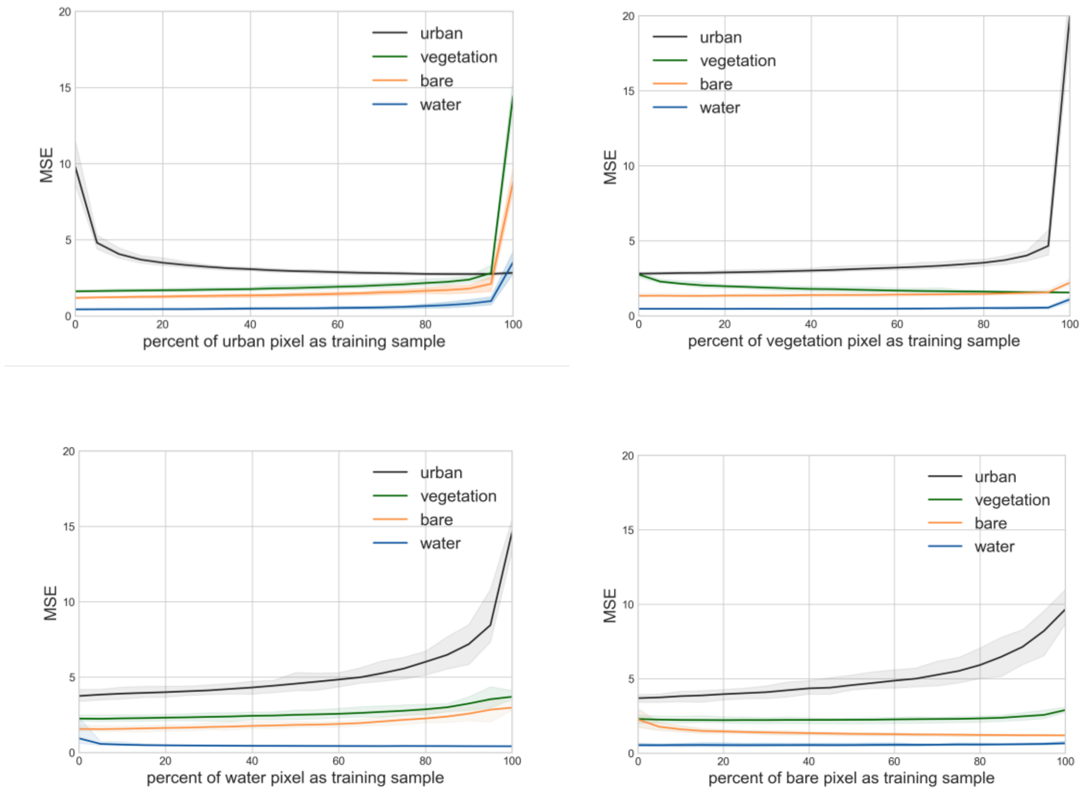

Figure 4.3. The influence of the percent of actual LULC sample pixels on the MSE of the random forest prediction results.

4.2.2 Data distribution

Before spatially evaluating the urban environment in Chengdu, it is useful to describe the distribution of the environmental indicators of the three dimensions for the purpose of exploring how individual indicator changed during the study period. Similar to box plot, violin plot has the function of visualizing data distribution. However, instead of mean, standard deviation, maximum and minimum shown in box plot, violin plot has the ability to visualize the probability density falling within certain values. Figure 4.4 shows the basic statistics about the individual indicators of all urban pixels and their dynamics in the four years.

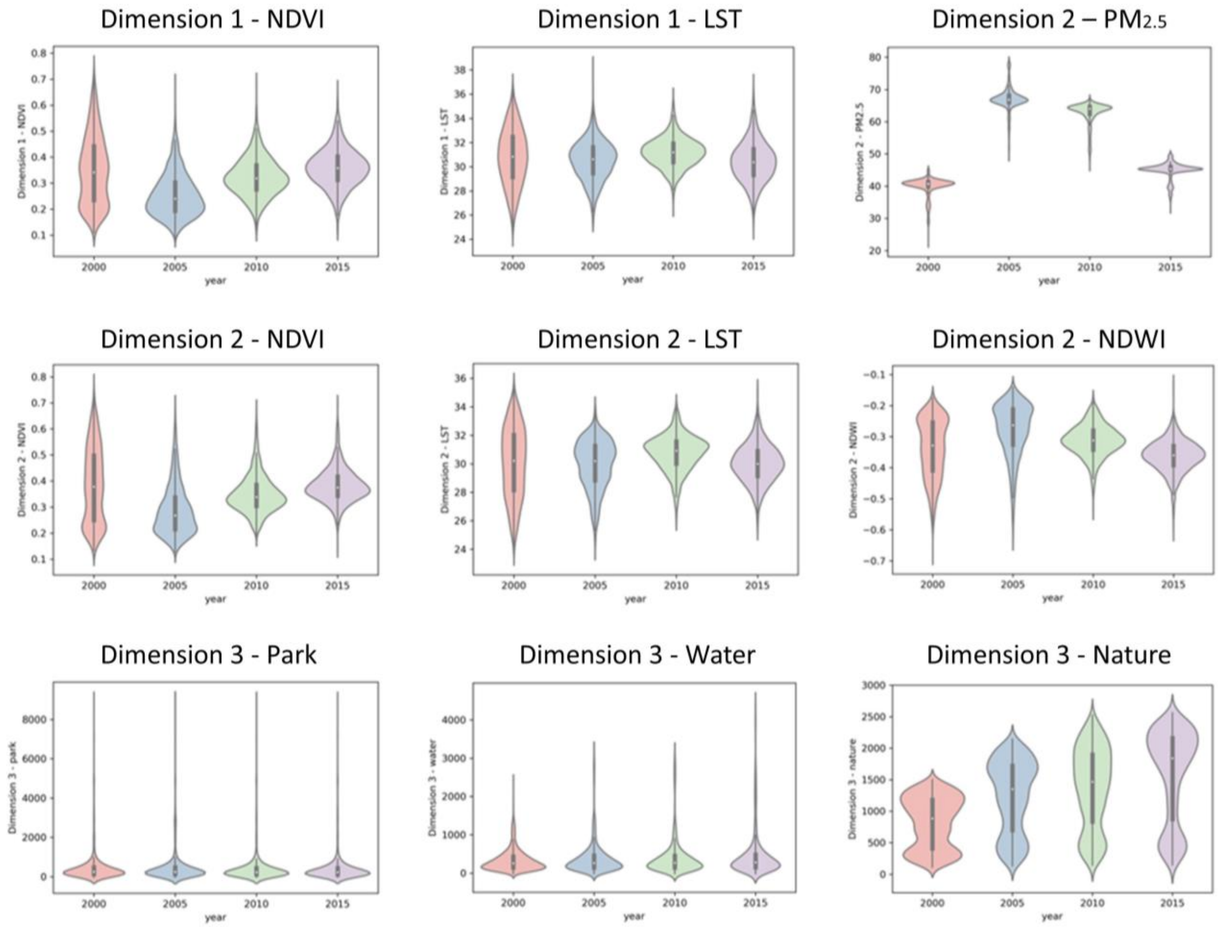

Figure 4.4. Violin plots of all urban environmental indicators in urban areas of Chengdu showing the dynamics of data distributions through time.

For the first indicator, urban greenness, in this study, is represented by NDVI calculated from satellite image and has a value ranging from -1 to 1. A higher value indicates a denser vegetation cover. In 2000, the NDVI values in all pixels had a widely-spreading distribution (i.e., a higher standard deviation) while the data were more compact in the other three years. In addition, in 2000, unlike the normally distributed histograms for other three years, there were two peak values, 0.2 and 0.35. Overall, through looking at the mean value and its changes, NDVI in Chengdu decreased from 2000 to 2005, but increased from 2005 to 2015.

For the composition of NDVI indicators, both Landsat 5 TM and Landsat 7 ETM+ data were used. Thus, the observed temporal trend may be due partially to the sensor difference between the two satellites. To verify the robustness of the results, the NDVI data obtained from the MODIS satellite were also plotted (Figure 4.5). Results from MODIS data demonstrated the consistency of temporal trends with the Landsat data, showing a small dip in 2005 during the study period. Although the trend of NDVI from MODIS was less obvious than that from Landsat, it might be due to the pixel mixture problem, since MODIS has coarser resolution than Landsat.

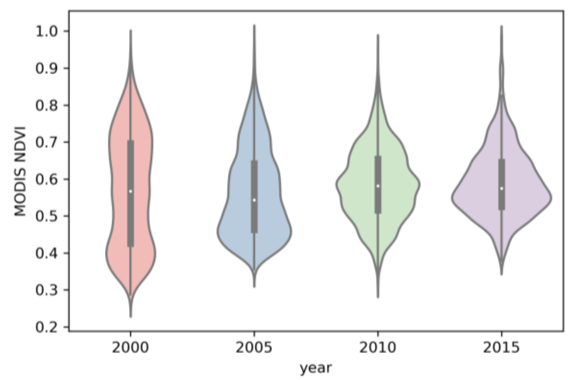

Figure 4.5. Data distribution of NDVI derived from MODIS data in urban areas of Chengdu.

LST is an important indicator of UHI, which influences residents' health. As seen in Figure 4.4, LST values in 2000 had a higher variation than those in the other three years. LST was negatively related to vegetation cover, so that the variation of LST is thought to have a reversed trend from NDVI. However, the mean value of LST in the urban area of Chengdu did not change much, approximately equaling to 30 degrees.

For $PM_{2.5}$, the range of the data was wide, but the standard deviation was low, and the histograms were generally skewed towards the higher values. The change of the $PM_{2.5}$ was prominent, showing an increase from 2000 to 2005 and then a decreasing trend to 2015. The lower tails were most likely comprised of the pixels located in the countryside.

Not only the greenness of each pixel but also the greenness in the neighboring regions play an important role in the urban environment for local residents. Neighboring NDVI in urban areas of Chengdu had the highest variation in 2000 but became lower later during the 15 years. The mean value of neighboring average NDVI decreased from 2000 to 2005 and then increased from 2005 to 2015.

The plot of neighboring LST values within Chengdu was similar to LST in the self dimension. The mean value of neighboring LST had no obvious change from 2000 to 2005, but increased during 2005-2010, and finally decreased from 2010 to 2015. The variation of data decreased from 2000 to 2010 and slightly increased from 2010 to 2015. Among the four years, the highest LST value was observed in 2010 and accompanied by the lowest standard deviation.

Calculated from remotely sensed images, NDWI can be used as an indicator for water content. Because there is limited water within the urban area, the average value of NDWI within certain regions fell below zero. The value of average NDWI within the neighboring region is positively correlated to the coverage of water in the neighboring area. The data distribution of NDWI in the urban area is also shown in Figure 4.4. The mean value of the neighboring NDWI increased from 2000 to 2005, and then decreased from 2005 to 2015. The data distributions in 2000 and 2005 were different from those in 2010 and 2015. In 2000 and 2005, the data distributions were skewed toward higher values. However, in 2010 and 2015, the data resembled normal distributions.

For the indicators in the accessibility dimension, a smaller value indicates higher accessibility. In the violin plot of accessibility to the nearest park, the distribution of park accessibility in all four years were skewed towards the lower values, meaning that most of the urban areas are close to their nearest parks, while outliers could have extremely long distances. There was a slightly increasing trend of the park accessibility values, suggesting that parks were becoming less accessible with time as urban expanded. However, the trends of mean value and variation were nuanced in the violin plot.

The distribution of water accessibility data showed a high and increasing data range while a relatively small and stable standard deviation. Similar to park accessibility, water accessibility was also skewed towards the lower values, and this phenomenon was most obvious in 2000. The mean values increased, albeit slightly.

The natural area is defined as the rural environment in this study. The data of rural environment accessibility had two peaks, one in the lower values and the other in the higher values. The mean value of this indicator gradually increased during the whole study period, as did its range and standard deviation. An increasing mean value indicates decreasing nature accessibility while increasing range and standard deviation suggested an increasing spatial disparity.

For all the nine indicators mentioned above, NDVI, LST and NDWI in self and neighboring dimensions had similar data distribution. Values on access to park and water had similar distributions. However, $PM_{2.5}$ and rural area accessibility had different data distributions from others. For NDVI, LST and $PM_{2.5}$, the worst situation occurred in the year of 2005. However, for NDWI, 2005 was the best year. The accessibility dimension is different from the other two dimensions, in which the value of the pixel was calculated based on the distance to specific objects. Therefore, it made the temporal change of three indicators in accessibility dimension different from the other six indicators.

4.2.3 Temporal trajectories of indicators

Figure 4.6 shows the temporal trajectories of urban environmental indicators (NDVI and LST) in the self dimension. The gray lines in the plots represent values in different counties, and the orange lines, blue lines and green lines refer to the mean values of counties in the central, peripheral and remote regions, respectively.

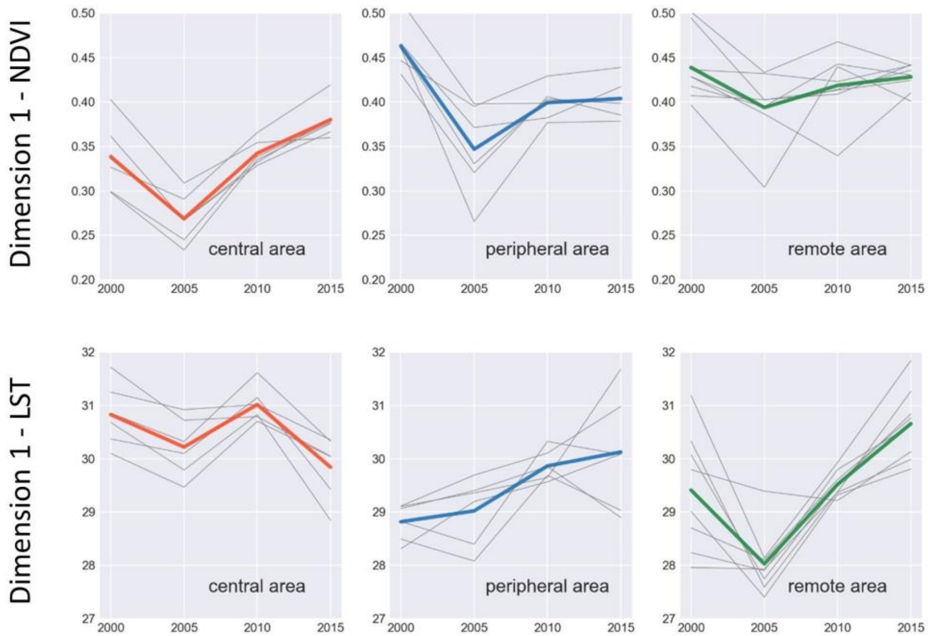

Figure 4.6. Temporal trajectories of indicators in the self dimension for the three different regions. Each gray line represents one county.

It can be seen that the central region had the lowest NDVI value but had the greatest increase over the 15-year period, from 0.34 to 0.38. The NDVI in the peripheral region decreased to a substantial degree during the first five years and then slightly increased. The remote region had the highest NDVI, but it was relatively stable throughout the whole study period. For each of the three regions, there was a dip of mean NDVI values in 2005.

Regarding counties in the central region, most of them had higher LST values than the peripheral and remote counties except for 2015 when the mean of LST in the central region achieved their lowest. The mean value of LST in all central counties decreased from 2000 to 2005 and from 2010 to 2015 while increased during 2005-2010. LST in the peripheral region increased stably during the 15 years. In the remote region, LST decreased from 2000 to 2005, followed by a sharp increase from 2005 to 2015.

The trajectories of indicator values in the neighborhood dimension were shown in Figure 4.7. For $PM_{2.5}$, all counties in all the regions were characterized by similar values and temporal trends. However, the $PM_{2.5}$ value of each county in the central region approximately equaled to the mean value of all counties in the central region. There were more variations in the other two regions, indicating that the counties in the peripheral and remote regions had more heterogeneous $PM_{2.5}$ values.

The change of neighboring NDVI had similar characteristics to that of NDVI of the self dimension. However, the overall value of neighboring NDVI was relatively higher than the NDVI value in self dimension. Among the three regions, the central region had generally the lowest neighboring NDVI values, while the remote region had the highest. The mean values in the remote area were relatively stable, but there existed obvious variations among different counties. For the central and peripheral regions, almost all of the counties had similar trends. However, in the remote region, no similar trend between different counties was identifiable in the line plot.

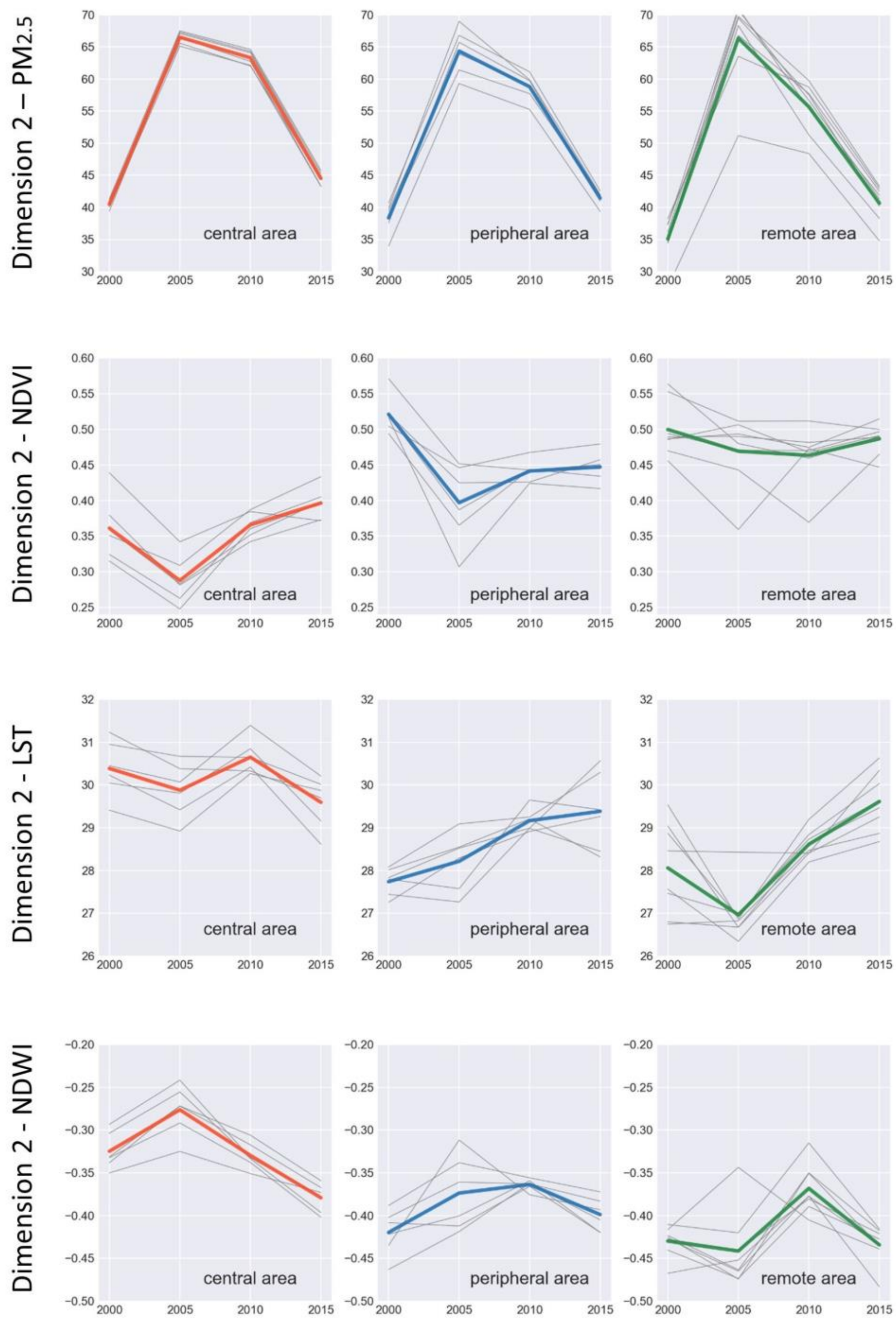

Figure 4.7. Temporal change of indicators in the neighborhood dimension for the three different regions. Each gray line represents one county.

The central region had the highest neighboring LST. During the study period, neighboring LST values in central counties first decreased and then increased. The final value in 2015 was lower than the initial value in 2000. The peripheral region was characterized by a trend of continuing increase. In the remote region, LST values decreased from 2000 to 2005, followed by a sharp increase from 2005 to 2015. Counties in the remote region had the least variation compared to the other two regions. In addition, counties in the central and peripheral areas have different changing trends.

The open water in central counties was higher than those in the peripheral and remote regions, and the values were higher in the peripheral region than those in the remote region. Except for the remote region, most central and peripheral counties experienced the first-increased-then-decreased trend. The change points for central counties were mostly in 2005, while 2010 for most peripheral counties. The value of neighboring NDWI in remote counties decreased from 2000 to 2005 and then increased from 2005 to 2010, and finally decreased from 2010 to 2015, except for one county.

Figure 4.8 shows the temporal change of indicators in each county in the accessibility dimension. For all indicators in this dimension, a higher value means poorer accessibility. The central region had the best park accessibility, followed by the peripheral region, while the remote region had the least. All of the three regions had decreasing trends of park accessibility. The differences between counties in the same region were pronounced, especially in the remote region.

Time cost to large open water surface in all three regions increased, meaning that accessibility to water decreased. Peripheral counties had the greatest increasing rate of time cost to water. In the beginning, time cost to large water surfaces in the peripheral and remote regions was almost similar and both higher than central counties. However, in 2015, the peripheral region had the highest time cost compared to the other two regions.

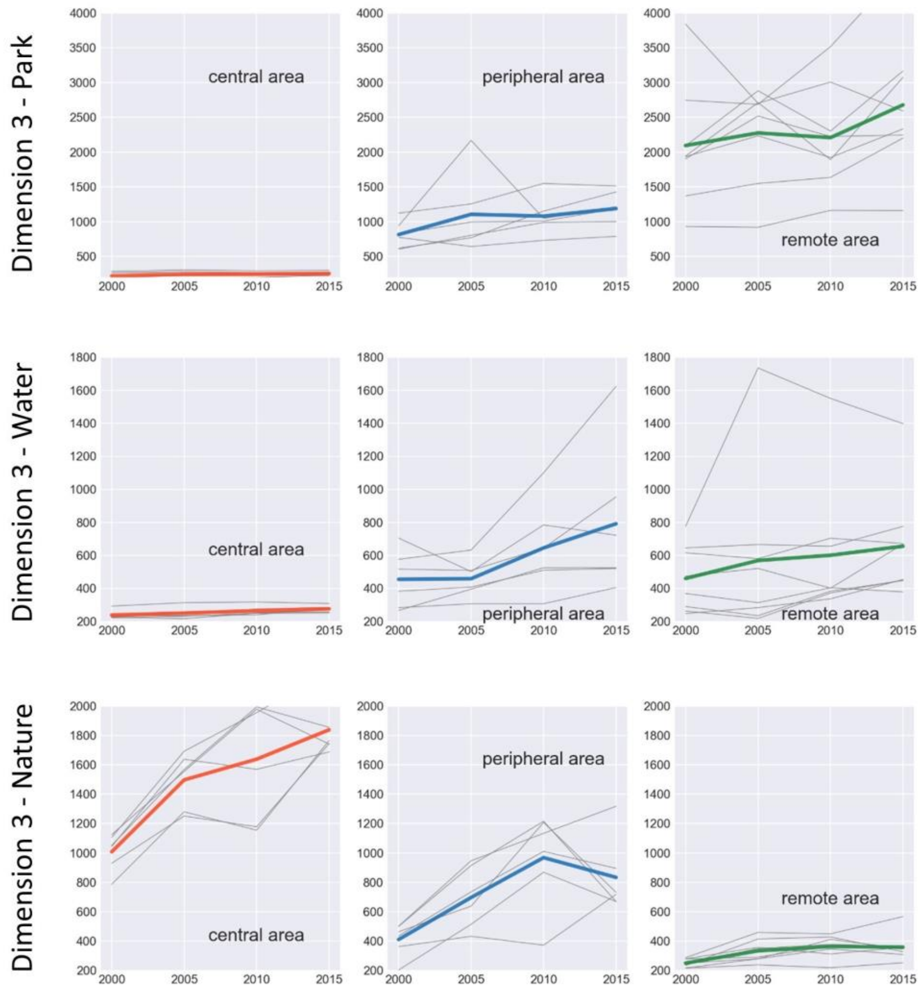

Figure 4.8. Temporal change of indicators in the accessibility dimension for the three different regions. Each gray line represents one county.

Central counties had the least access to nature, followed by the peripheral region. The remote region had the finest access to natural land. Central counties also had the greatest decreasing rate of accessibility. Accessibility in the peripheral region had a decreasing trend during

2000-2010, but an increasing trend during 2010-2015. Among all the three regions, counties in the remote region had the most similar temporal changes to each other.

In summary, central counties had very different temporal trends from the counties in the other two regions. The variation between different counties within one region suggested that a central county was more similar to another, while peripheral and remote counties were more heterogeneous. At the same time, central counties had greater trends towards a better urban environment based on the analysis of individual indicators except for NDWI and $PM_{2.5}$.

4.3 Urban environmental evaluation

As described in section 3.6, indicators in each dimension were aggregated together to represent the environmental condition in that dimension. Then, the results of environmental evaluation in the three dimensions were aggregated to represent the overall evaluation of comprehensive urban environment in Chengdu. There was no pre-defined threshold in the study to distinguish which place had definite good or poor environment, and the absolute scale of the score was of little means. However, the results were given to show the relative environmental condition of one location compared to another within the whole study area of Chengdu, and the same location at a certain time compared to another time. For the results of three dimensions and the overall comprehensive evaluation, a higher value represents a better environment. In the maps, the brown color denotes a relatively poor environment, while green means a relatively favorable environmental condition. The borders of the central, peripheral and remote regions were delineated using the black line, gray line and dashed gray line, respectively.

4.3.1 Self dimension

The self dimension of the urban environment is a comprehensive value of NDVI and LST at the pixel level of the study area. The values in this dimension are spatially mapped in Figure 4.9

for the four years. The overall trends of environment condition in this dimension decreased from 2000 to 2005, and then increased from 2005 to 2015. In 2000, the urban center of Chengdu had the lowest value, representing a relatively poor urban environment, compared to the other areas. However, with time, this center-outer disparity effect tended to fade out, as shown by more spatial coherence from central to remote regions in Chengdu. The self dimension of the urban environment was the least favorable in 2005, while the best in 2015.

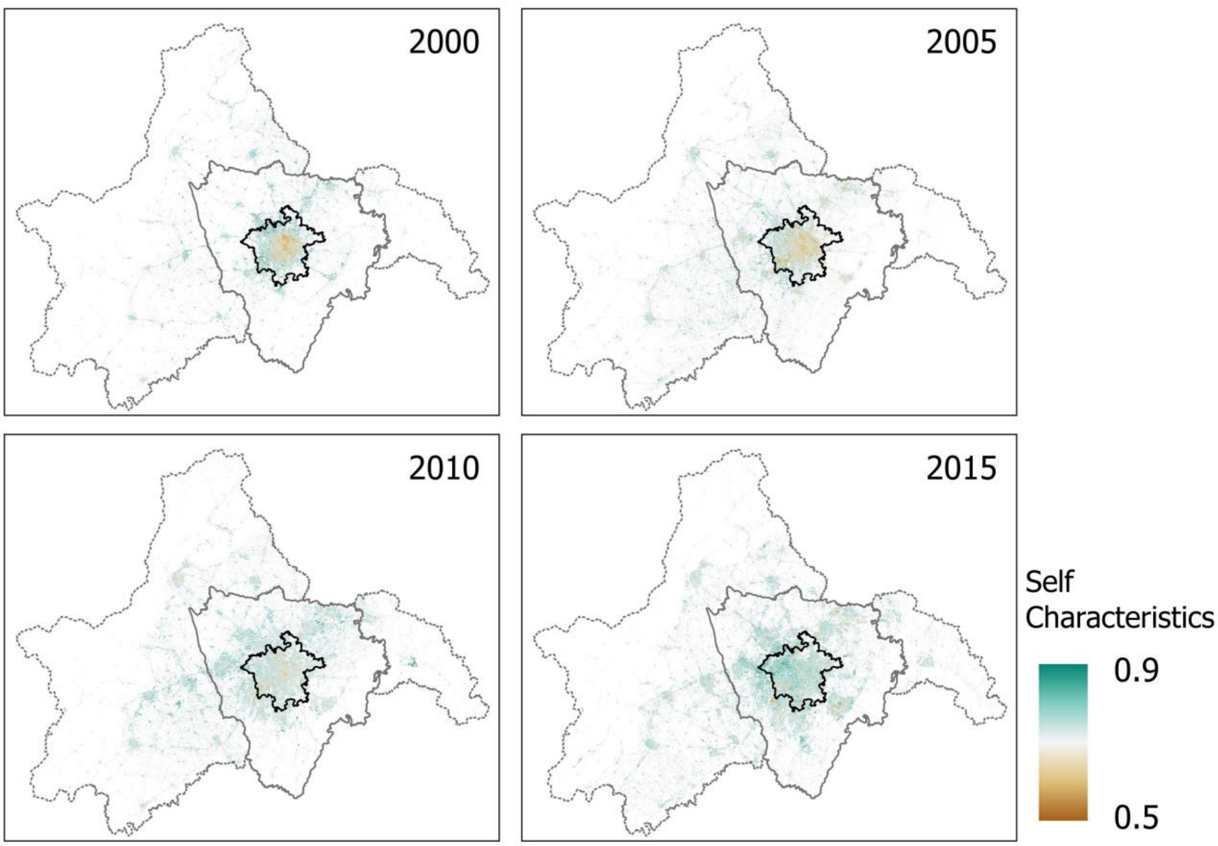

Figure 4.9. Spatial patterns and temporal dynamics of the urban environment in the self dimension.

4.3.2 Neighborhood dimension

The result of the neighborhood dimension (Figure 4.10) had a similar trend to the change of the urban environment in the self dimension. It also followed the trend of decrease from 2000 to 2005 and increase from 2005 to 2015. The center-outer disparity phenomenon is obvious in the years of 2000 and 2010, while the neighboring urban environment in 2005 in almost all area was at a relatively poor condition. In 2015, the environment in all places of Chengdu changed back to a favorable condition, which is as good as the year of 2000, except for some industrial areas in the northeastern part of the peripheral region (in Longquanyi county).

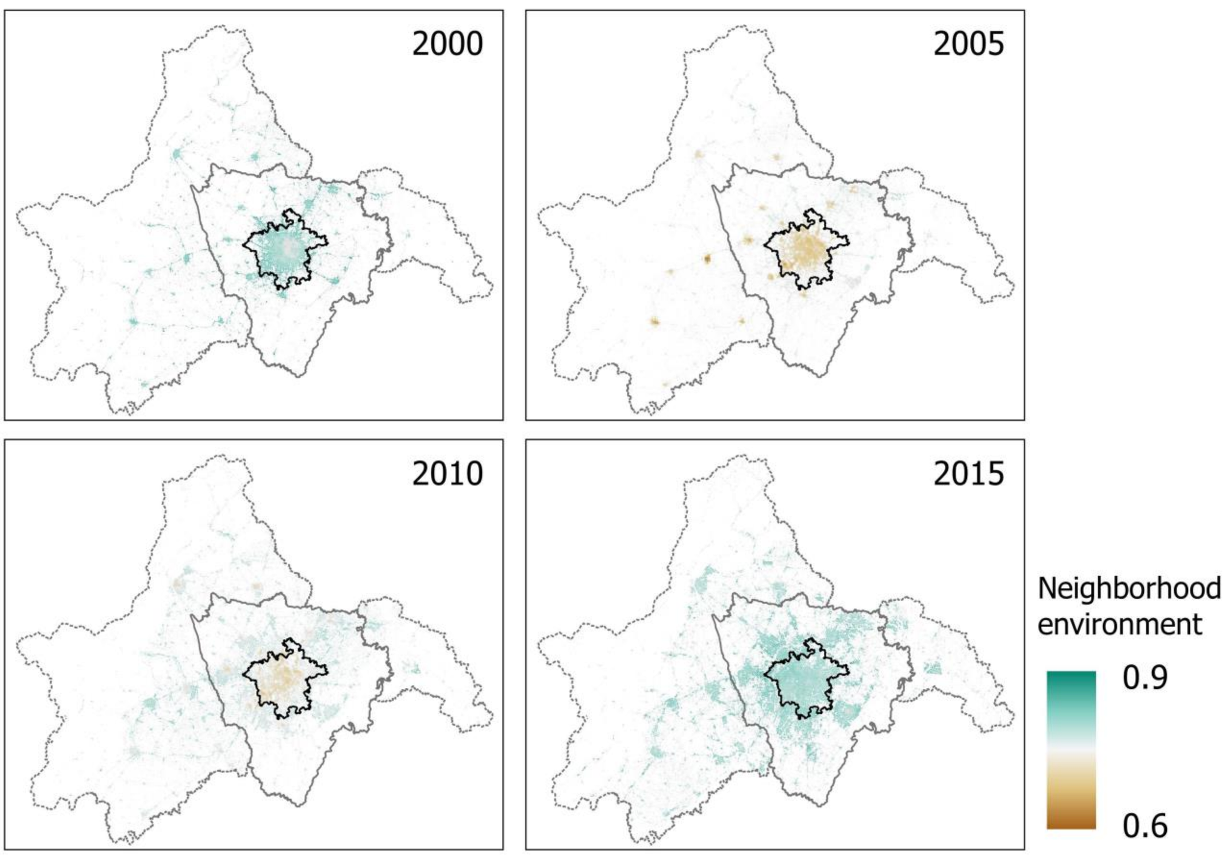

Figure 4.10. Spatial patterns and temporal dynamics of urban environment in the neighborhood dimension.

4.3.3 Accessibility dimension

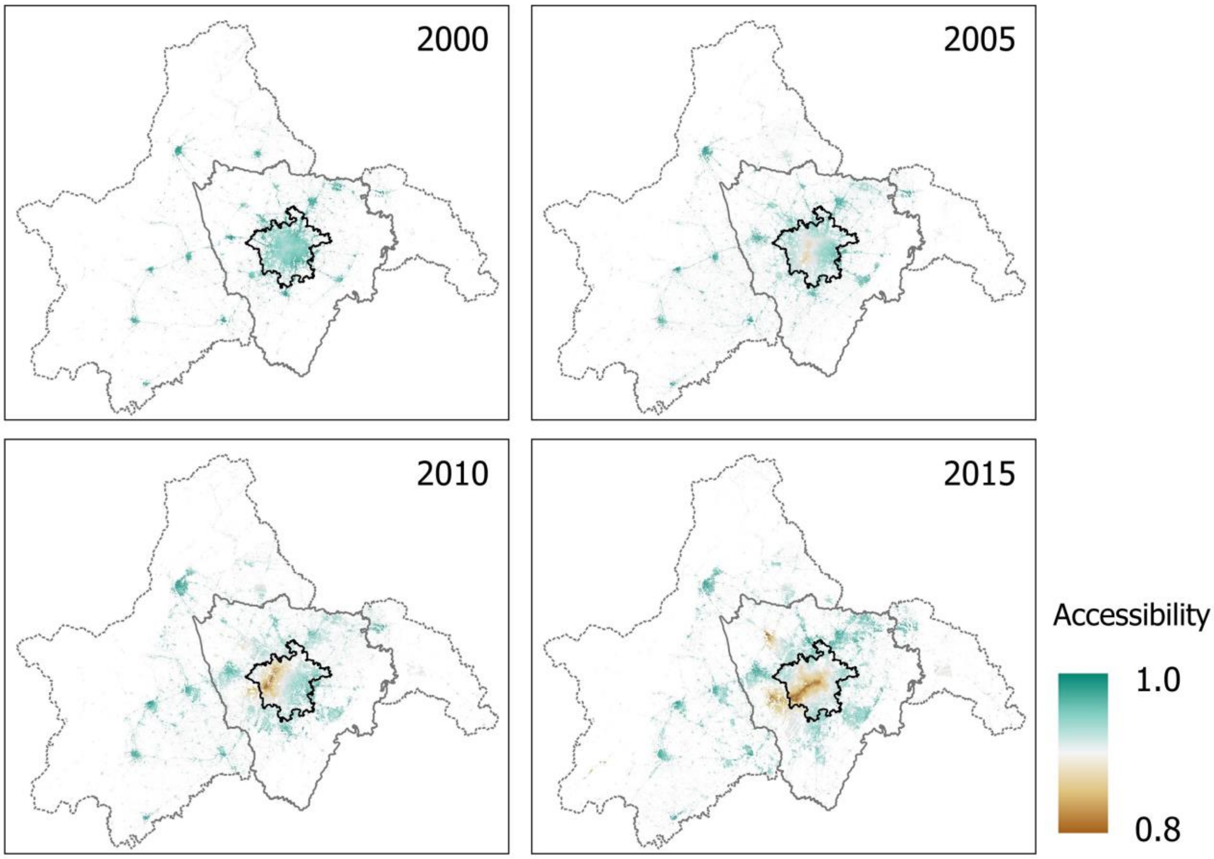

Figure 4.11. Spatial patterns and temporal dynamics of urban environment in the accessibility dimension.

The accessibility dimension of the urban environment had a pattern that was distinguishable from those of the other two dimensions, since the aim of designing this dimension was different. The first and second dimensions considered the environment where people live, while this dimension considers access to urban natural or anthropogenic environmental infrastructure such as parks. Expanded urban areas of the Chengdu were most likely located in the urban fringes, and the urban center went through a trend of continuing decline of nature accessibility. For those small urban clusters in the peripheral and remote regions, the values did not substantially change. However, from 2000 to 2015, the accessibility condition in the central part of Chengdu deteriorated, manifested by the growing brown areas. The worst situation was in the southwestern part of the central area, in which most of the urban extensively expanded.

4.3.4 Integrated evaluation at 3-dimensional coordinate system

The urban environment evaluation value of all three dimensions was plotted for the four years to understand the environmental condition dynamics in the three dimensions and their relation through exploring the distribution of data and the changes. The orange, green, and blue dots represent pixels in the central, peripheral, and remote regions, respectively. The wider the scatter of the data points along each of the three axes, the greater the spatial disparity in that dimension.

The distribution of the environmental evaluation values in the 3-dimensional (3-D) system changed in four study years, although those shapes in 2000 were similar to 2005, and those in 2010 was similar to 2015 (Figure 4.12). In 2000 and 2005, the urban environmental evaluation values in the central region widely scattered along the self dimension while they were relatively compact in the neighborhood and accessibility dimensions. This formed a cigar-shaped cloud in the 3D coordinate system. In 2010 and 2015, the cigar-shaped cloud became oval-shaped with the range of values in the neighborhood and accessibility dimension elongated. The shape and changes of value points in peripheral and remote regions were similar; they were normally distributed along three axes (slightly stretched along the self dimension) forming an oval-shape and gradually became more scattered. One more thing to mention is that pixels in the central and remote regions had higher values in the accessibility dimension in 2000 and 2005. However, the values of accessibility dimension in the peripheral region were higher in 2010 and 2015.

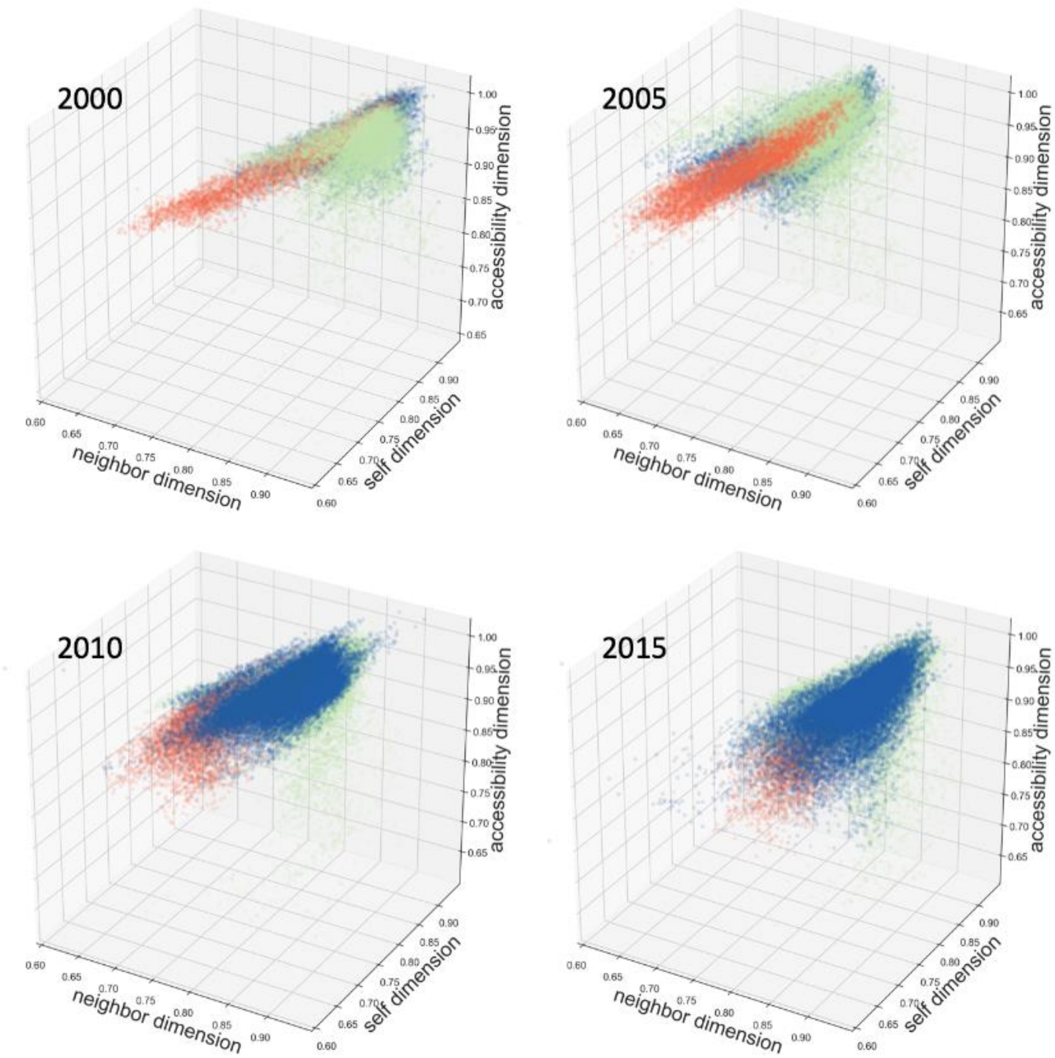

Figure 4.12. Three-dimension scatterplots of the urban environment in Chengdu. The shape and dynamics of data values in the three regions were different.

4.4 Comprehensive evaluation of the urban environment

The results of the urban environmental evaluation are summarized in Table 4.5. For the self dimension, the mean value of urban environment slightly decreased from 0.7639 in 2000 to 0.7387 in 2005, then bounced back to 0.7633 in 2010, and continued increasing to 0.7725 in 2015. The mean value of the neighboring dimension followed a similar trend, but it (0.8178 in 2015) did not reach the original highest state of 0.8242 in 2000. The mean value of the accessibility dimension experienced a continuing decrease from 0.9572 in 2000, to 0.9383 in 2005, to 0.9277 in 2010, and finally to 0.9213 in 2015. The comprehensive dimension of the urban environment is an integration of the values for the three dimensions and represents the overall urban environmental change during the study period. The comprehensive value in 2000 is 0.9296, and it then decreased to 0.9099 in 2005, nearly stably increased to 0.9191 in 2010, and finally increased to 0.9269 in 2015 similar to the value in 2000. The dynamic suggested that the urban environment in Chengdu went through a process of degradation from 2000 to 2005. Afterward, the environment of Chengdu improved, albeit never achieved the original best state in 2000.

Table 4.5. Results of comprehensive urban environmental evaluation

Dimension	Statistics	Year 2000	Year 2005	Year 2010	Year 2015
Self dimension	Max	0.9968	0.9635	0.9551	0.9585
	Mean	0.7639	0.7387	0.7633	0.7725
	Min	0.5594	0.4642	0.5854	0.2008
	Std. Dev.	0.0784	0.0678	0.053	0.0537
Neighborhood dimension	Max	0.904	0.8322	0.8501	0.8697
	Mean	0.8242	0.7293	0.7631	0.8178
	Min	0.7229	0.6203	0.6792	0.6013
	Std. Dev.	0.0353	0.0315	0.0314	0.0196
Accessibility dimension	Max	0.9923	0.9909	0.99	0.9899
	Mean	0.9572	0.9383	0.9277	0.9213
	Min	0.6661	0.5654	0.7588	0.6575
	Std. Dev.	0.0192	0.0278	0.0356	0.0417
Comprehensive evaluation	Max	0.977	0.9597	0.9689	0.973
	Mean	0.9296	0.9099	0.9191	0.9269
	Min	0.8782	0.8617	0.8371	0.8295
	Std. Dev.	0.0177	0.0147	0.0134	0.0116

At the spatial scale (Figure 4.13), the disparity of the urban environment was mainly characterized by the distinction between the urban center and outskirts in 2000 and 2005. After 2005, the situation of disparity was alleviated and became homogenous in 2015. With the urban center of Chengdu became better, the urban area in the surrounding counties, namely those located in the peripheral and remote regions, had degraded to some extent.

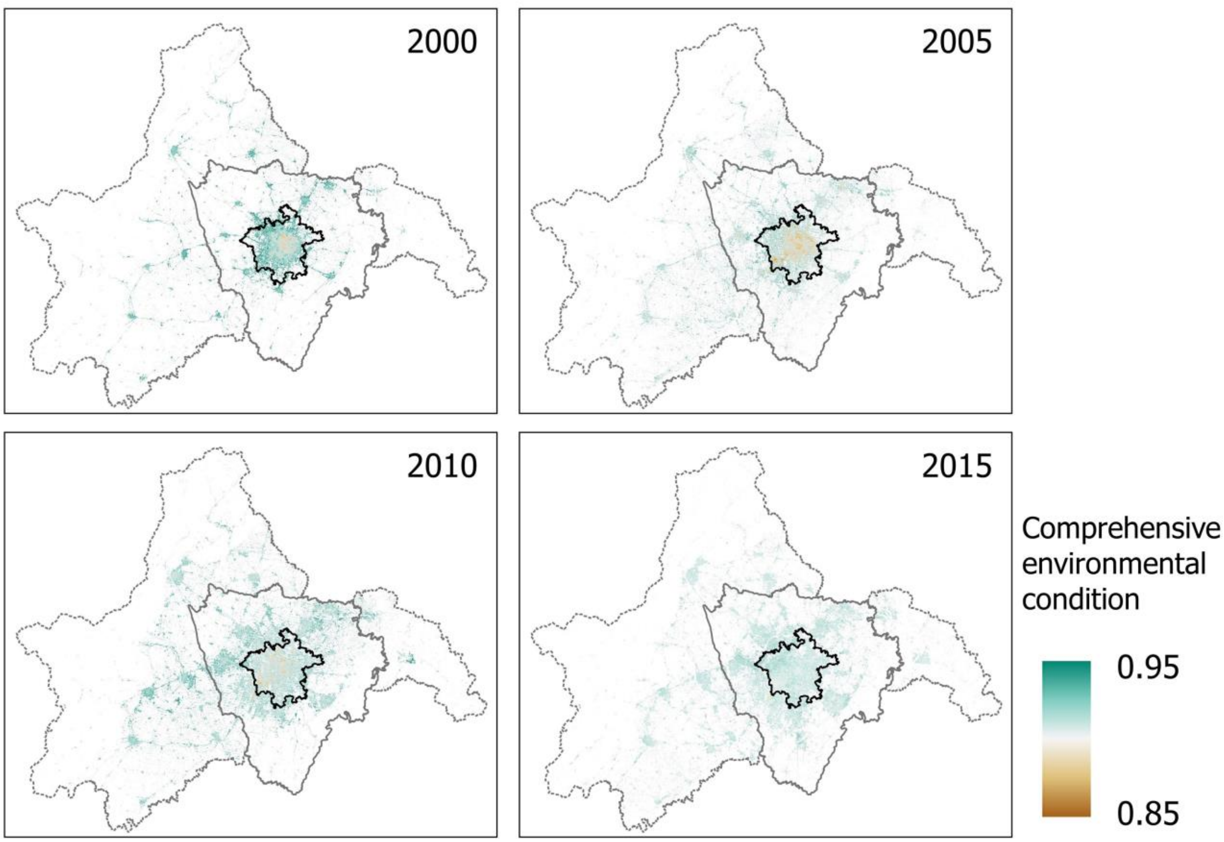

Figure 4.13. Spatial patterns and temporal dynamics of the comprehensive urban environment evaluation.

The mean value of the four-years comprehensive environmental condition in each county was calculated and mapped to understand the ranking of the relative environmental condition of the counties using the equal quantile classification method. According to Figure 4.14, all the counties with the very good environmental condition were in the remote region, while all the counties with the very poor environmental condition are in the central region. Counties in the peripheral area have good, fair and poor environmental conditions.

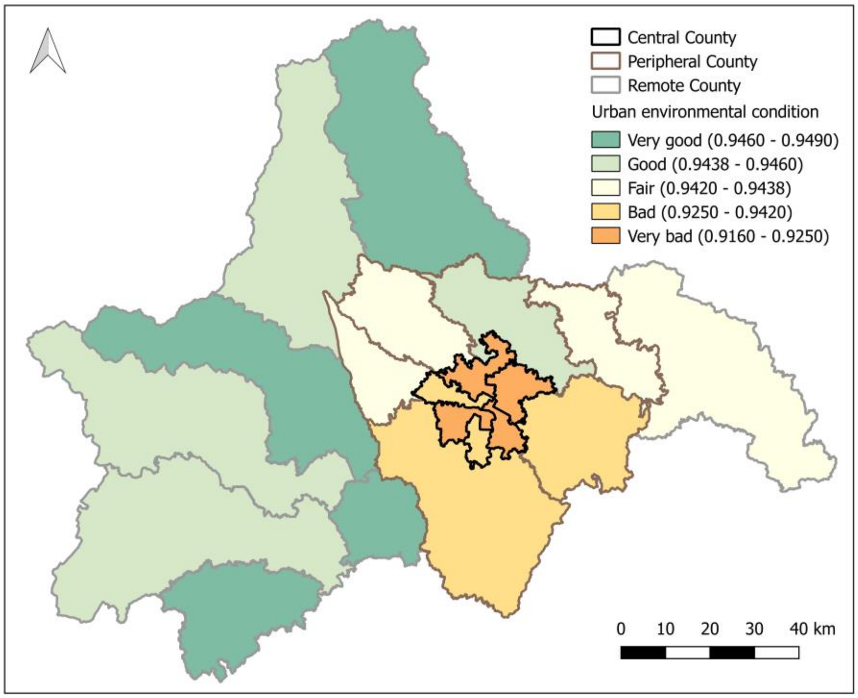

Figure 4.14. Spatial and temporal averaged comprehensive environmental condition of all counties in Chengdu. The categories were defined using the equal quantile method. In Chengdu, in the past 15 years, the worst environmental condition was in the central region while the remote counties had a relatively good condition.

The changes of urban environmental condition (Figure 4.15) revealed a different spatial pattern from the mean of environmental condition. There was no obvious difference between central counties, peripheral counties and remote counties. One of the most prominent patterns is that the counties to the west of the urban core were highly degraded. This was coincident with urban expansion results that the western adjacent part of the urban core experienced the most urban expansion. Another thing to mention is that no counties that are separated from central core by mountains were degraded or highly degraded.

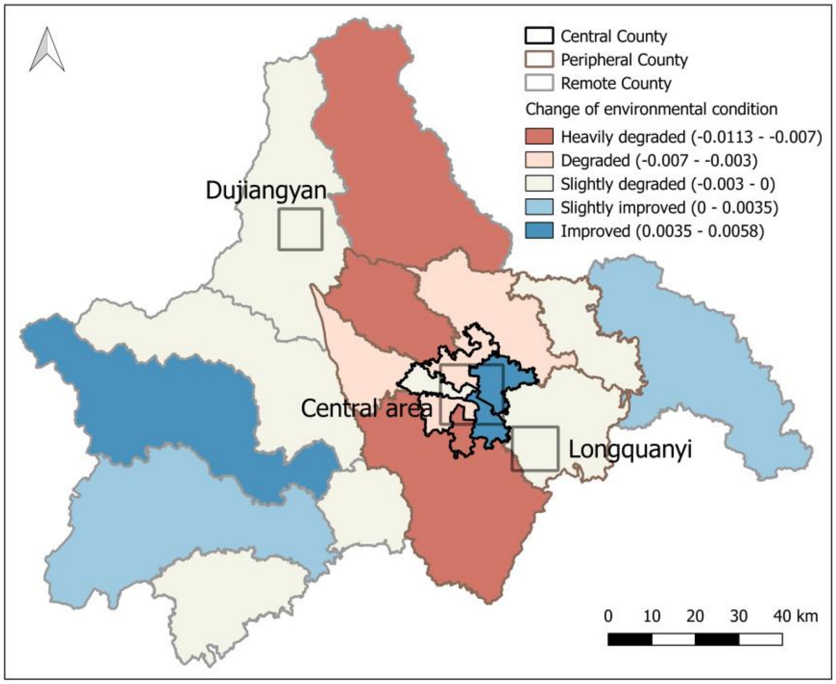

Figure 4.15. The change of comprehensive environmental condition of all counties in Chengdu calculated by subtracting the mean of the previous two years (2000 and 2005) by the mean of the latter two years (2010 and 2015). The western counties adjacent to the urban core were highly degraded while counties to the east and most of the remote counties were improved.

Table 4.6 provides information about the change of the relative environmental condition within the county through time. From 2000 to 2005, all counties had degraded urban environment, while the degradation degree in the central and peripheral regions were much higher than that in the remote region. During 2005-2015, almost all counties experienced an improvement of environmental condition, except for Shuangliu, Pixian, Pengzhou in 2005-2010 period, and Qingbaijiang, Dayi in 2010-2015 period. Those deteriorating area during 2005-2015 experienced relatively faster urban expansion than many other counties.

Table 4.6. Change of comprehensive environmental condition at counties of Chengdu.

County	2000 - 2005	2005 - 2010	2010 - 2015
Jinjiang	-0.0201	0.0132	0.0052
Qingyang	-0.0187	0.0001	0.0161
Jinniu	-0.0249	0.0017	0.0152
Wuhou	-0.0296	0.0021	0.0119
Chenghua	-0.0253	0.0124	0.0081
Gaoxin	-0.0258	0.0032	0.0038
Longquanyi	-0.0286	0.0106	0.0035
Qingbaijiang	-0.0231	0.0121	-0.0038
Xindu	-0.0256	0.0049	0.0048
Wenjiang	-0.0194	0.0015	0.0085
Shuangliu	-0.0221	-0.0009	0.0042
Pixian	-0.0179	-0.0054	0.0061
Jintang	-0.0187	0.0097	0.0007
Dayi	-0.0127	0.0116	-0.0030
Pujiang	-0.0103	0.0014	0.0067
Xinjin	-0.0171	0.0048	0.0016
Dujiangyan	-0.0116	0.0004	0.0065
Pengzhou	-0.0157	-0.0034	0.0072
Qionglai	-0.0108	0.0084	0.0000
Chongzhou	-0.0236	0.0110	0.0009

To have a detailed analysis on the spatial distribution of urban expansion and the urban environment at the pixel level in different regions of Chengdu, three zoomed-in illustrations of the rectangular regions are provided, including Longquanyi in the peripheral region, Dujiangyan in the remote region and all counties in the central region. The regions were chosen in order to show the result of pixel-based environmental valuation (Figure 4.16). The overall environmental condition in the central area went down from 2000 to 2005 and got better thereafter. The clusters of degraded areas in the center became less prominent and the whole area became more heterogeneous over time. The relatively good environmental condition in Longquanyi and Dujiangyan degraded during the 15-year time period. Although conditions in the newly expanded urban area of these two regions were favorable, the old town area was rapidly degraded.

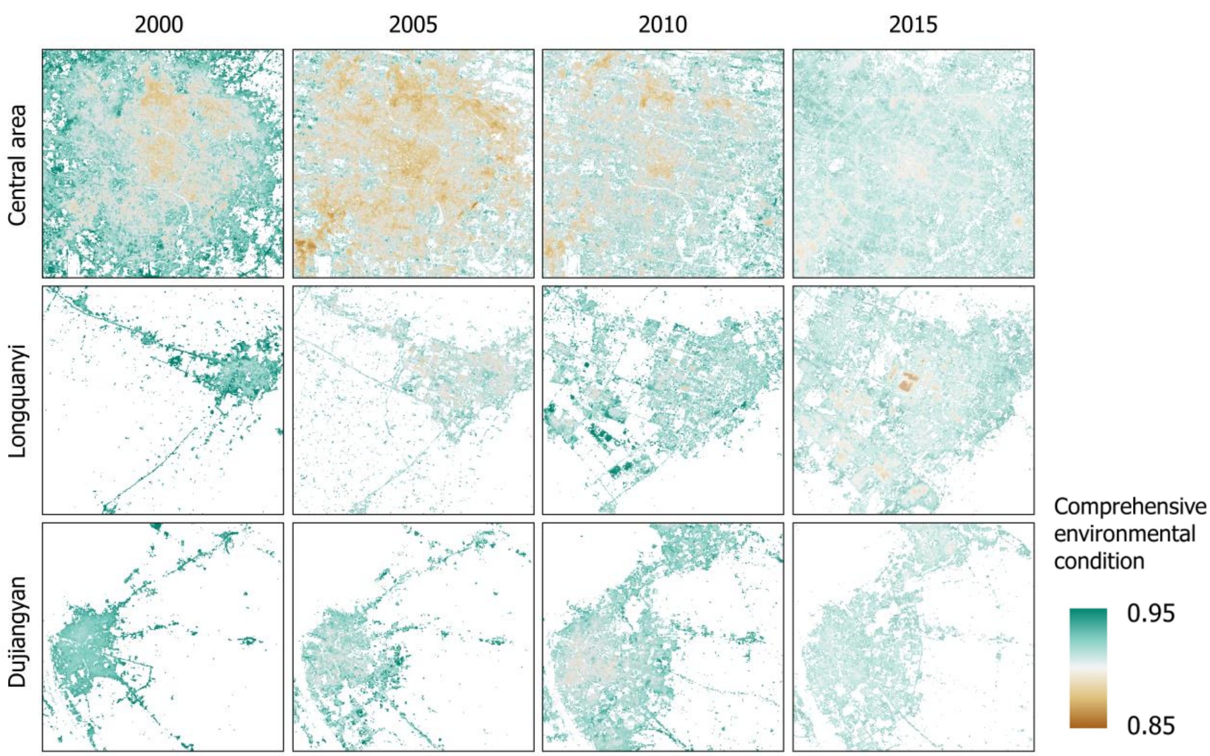

Figure 4.16. Comprehensive evaluation of urban environmental condition in three sub-regions.

4.5 Urban environment and urban expansion

The regression result between the urban environment and urban expansion is shown in Figure 4.17. The fitted three univariate models have similar slopes, which are -1.38×10^{-4}, -9.14×10^{-5}, -8.64×10^{-5}, all around -1×10^{-4}. It reflects that with every one square kilometer increase of expanded area, the change of urban environment decreases by 1×10^{-4}. This suggests that urban expansion may have a negative effect on the urban environment. The P values of the independent variable in the linear model are 0.317 for 2000-2005, 0.231 for 2005-2010, and 0.188 for 2010-2015, all of which are insignificant. According to this result, although we can say that the increase speed of expanded urban area may have a negative consequence on the change of urban environment, it is not statistically significant to reject the null hypothesis.

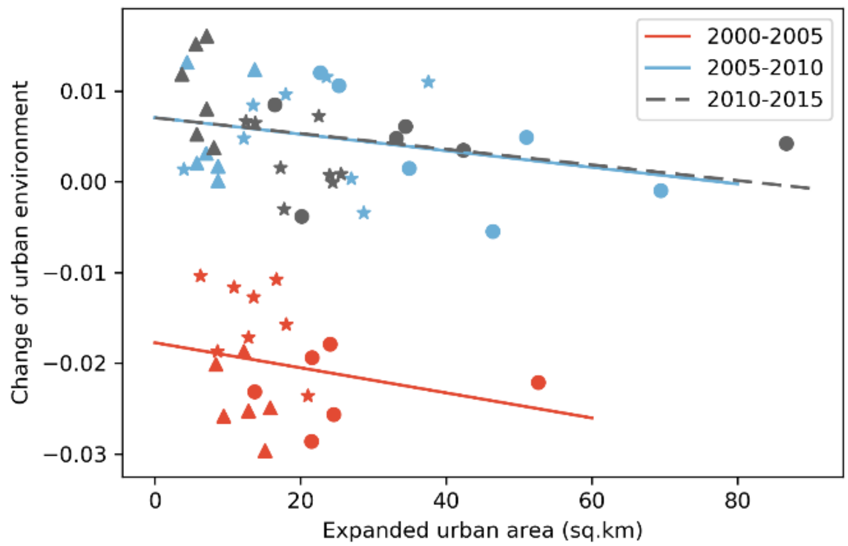

Figure 4.17. Regression between expanded urban area and change of urban environmental assessment value. The star signs stand for central counties, circles for peripheral counties, and triangles for remote counties.

CHAPTER 5: DISCUSSION

5.1 Drivers and Policy implications

In this research, not only the temporal-spatial distribution of urban expansion and urban environmental dynamics but also the uneven development between different counties are analyzed. In addition, the factors driving the changes directly, indirectly or unintentionally are discussed according to the results. The spatial and temporal pattern of urban expansion and urban environment in Chengdu are shaped by many factors including government policies, market forces, and geographic and social background of different areas.

5.1.1 Government policies

The main driver of urban development in Chengdu is the implementation of government policies. The accelerated speed of urban expansion after 2000 resulted primarily from the implementation of the "Go West" program by the Chinese government (Schneider et al., 2005). To achieve balanced development between the western and eastern parts of China, the national government established several strategies in western provinces to promote the economy, livelihoods, infrastructure, education, public health, etc. As one of the hotspots of this program, Chengdu, the capital of Sichuan Province, has witnessed a rapid rate of increase in population and infrastructure construction. Stimulated by the flourishing economy and consequently more job opportunities, growing population, and increasing housing needs, the urban area has rapidly expanded (Peng et al., 2015).

The process of urban expansion in peripheral and remote regions of Chengdu is prominent during the periods of 2005-2015. This may result from the implementation of two policies. One is the "Small-City Strategy" that promotes the development of neighboring small cities, towns and counties around the center of large cities to avoid overcrowding (Chen & Gao, 2011). The other is the “Coordinated Development between Urban and Rural Sectors” (Chen et al., 2011; Ye et al., 2013), which is a strategy by the central government aimed at helping the rural population to settle in urban areas, especially small cities and towns. Since the government implemented the “Coordinate Development” strategy, the proportion of non-agricultural population in Chengdu had grown from 37% in 2003 to 53.7% in 2007 (Chen and Gao, 2011), and the migrants from rural to urban areas increased the demands for residential housing, especially in small satellite cities/towns/counties around the centers of big cities, accelerating the urban expansion.

Along with economic development, the local government started to consider environmental protection to build a better living place for the residents. With the idea of building a “garden city and village” (Ai and Huang, 2010) implemented by the city government, the creation of a good living environment became one of the central goals of city planning in Chengdu (Zhao and Yang, 2016). The planting and protection of trees along the road and the design of landscape inside the residential area made the urban environment in Chengdu greener.

5.1.2 Market forces

With the reconstruction of the economy and the inflow of global capita (Yue et al., 2014), the inland cities experienced rapid economic reform following the developing pace of coastal cities. The emergence of manufacturing and high-tech industries infills the city with the migrated population. The planning of main types of construction and different functional buildings was designated for each county in Chengdu and thus the expansion was uneven for counties in different time period.

Before 2000, to promote economic development, the investment highlights the development in the second sector, especially manufacturing. Many factories were built in the east of the central region. After the implementation of policies such as “Go West” and “coordinate development", the housing needs increased, and the real estate industry flourished, promoting the construction of residential buildings that favors the well-maintained southwest of the city. At the same time, with the designation of high-tech zones in the south of Chengdu, the economy was shifted to the tertiary sector so that the many national and international companies rooted in southern Chengdu (Schneider et al., 2005), leading to the construction of malls and complexes in Gaoxin district.

The environmental changes are also driven by market forces, led by the real estate industry. To accommodate the increasing population and provide a better environment within communities with a higher price of realty, low-rise buildings were demolished and changed to high-rise buildings. This not only provided more housing opportunities but also left more space for designing landscape in the residential area, thus increasing the green cover and alleviating the urban heat island effect. This phenomenon was prevalent in the central region of Chengdu, where many old buildings were demolished or reconstructed.

Apart from the good effects, there was also an air quality issue in this city. To stimulate the economy, environmental protections were neglected by the government for years. The rapid urban construction and development of heavy industry polluted the air in Chengdu. Although factories were required to move to the outskirts where there are fewer residents, wastes from factories (industrial facilities) were still one of the main sources of air pollution (Qiao et al., 2015). At the same time, the waste gas from vehicles resulting from busy transportations and the burning of biomass in rural areas intensified the air pollution (Chen et al, 2014).

5.1.3 Geographic and social background

The geographic condition is one of the main reasons for the finding that most peripheral counties were less urbanized. The two mountain ranges standing to the west and east of Chengdu form the basin of Sichuan. The soil is fertile in the central basin while barren in the mountainous areas. The mountains also decreased the accessibility to the central urban area through transportation. Therefore, the peripheral regions in the east and west of Chengdu were less expanded by urban areas.

For the other counties such as Chenghua, their urban areas were less expanded because of the social background. In the early 2000s, the construction of factories driven by industrialization was concentrated in the eastern part of Chengdu, which made this part less favorable to permanent residents. Therefore, the urban area in the eastern part of the city was less expanded when the real estate industry flourished. At the same time, a large portion of the newly constructed urban areas during 2010-2015 was built to the south of the central counties. This may be due to the development of "New Tianfu District", which aimed to attract investment by private sectors (Liu and Jin, 2012). These planning strategies have accelerated the increase in urban land use of Chengdu mainly occupied by domestic and international companies.

With the rapid expansion, the old town area went through continuing degradation in terms of accessibility to the natural environment, because most of the expansion happened around the fringe. At the same time, the high cost of reconstruction in populated old blocks prevents the building of green and blue infrastructures. These are the main reasons for the result that some old urban areas were degraded in accessibility dimension. As the government and companies care more about environmental protection when doing construction nowadays (Legates & Hudalah, 2014), it is recommended that green and blue infrastructures should be well planned before building the community. Finally, greater strength of building and updating the infrastructures should be put on the southwest side of the city where the expansion speed was relatively high.

5.2 Linking urban expansion and urban environment

As the urbanization process continues, the world is now facing challenges from human impact on land use change in addition to global climate change (Seto & Satterthwaite, 2010). The rapid urbanization has profound effects on the environment, reflected in three ways: 1) directly in the living environment inside the city itself; 2) in the adjacent environment that urbanization process gradually prevails; 3) to the remote places that telecouple with and sometimes burden the consequence of pollution from the city. The environment inside the city, which is chosen as the topic in the present research, has the most direct relationship with human beings because it influences the health of residents. Based on the regression analysis in this study, it can be seen that rapid urban expansion may have negative consequences on the urban environment. However, based on the analysis of urban environmental change map, different areas in Chengdu represent different patterns regarding the relationship between urban expansion and urban environment. Generally, if no planning strategy is implemented to improve the old town area, with the urban area expanded along the edges (the most typical situation in China), it can be expected that the urban environment would degrade, and it is noticed to be true in the old town area of many counties of Chengdu in the present research. However, the counties in the central region of Chengdu is an exception. There is an obvious improvement of the environment in the urban core of Chengdu in 2015, mainly resulting from government policies and market forces as previously discussed.

Researchers have explored the relationship between urban expansion and urban environment in many studies. Zhao et al. (2006) found negative environmental consequences of rapid urbanization in Shanghai. He et al. (2014) illustrated the negative consequence of economic development with the focus on environmental degradation through pollution in China. Yue et al. (2014) found that the economic development and therefore urban expansion is highly interrelated with the urban environment at the district level in Shanghai. The study of Vietnam (Fan et al., 2019) shows that urbanization contributes to environmental deterioration. The present study suggests that while the rapid urban expansion will lead to a degraded urban environment, this relationship will be broken through the implementation of environmental policies. With strong policy intervention on environmental protection, the negative consequences caused by the rapid urban expansion will be alleviated.

5.3 Caveats and future directions

This study has caveats and limitations. First, the sampled pixels for urban extraction and validation are limited by the availability of fine resolution images from Google Earth, and for some places and times with no high-resolution images, the image itself was used as reference (Zhu & Woodcock, 2014). This reduced the classification accuracy. Additionally, the urban expansion area summarized in Figure 4.2 is under the assumption that urban expansion is irreversible through the study period 2000-2015, which would cause overestimation in urban areas (represented by impervious surface), albeit to some trivial degree. Second, the selection and definition of urban environment indicators are subjective and constrained by data, which influence the effectiveness of representing the overall urban environment in Chengdu. Through incorporating more relevant environmental indicators suggested by many researchers (Li et al., 2009; Shen et al., 2011), future studies can refine the model to achieve better evaluation. Third, the assessed values of the three dimensions and the final comprehensive results are relative scores of urban environments. Thus, the status of “improve” or “degrade” means the relative change of urban environment across the study period. Nevertheless, although the scores may change with the processing of data with different data scales, the general pattern of spatial and temporal dynamics should be identical within the same study periods as other researchers did (Su et al., 2011, Zhou et al., 2018). Fourth, the linear regression model between urban expansion and urban environment does not take into account of the error propagation originated from image processing, classification, indicator calculation. Last, the urban expansion is analyzed only to the horizontal direction in this study while the vertical direction is also an important dimension to study especially in megacities such as Chengdu.

This study focuses on exploring the spatial and temporal dynamics of urban expansion and the urban environment, and analyzed their relationship using a simple linear model. However, the complex processes and mechanisms between urban expansion and environment are beyond the scope of this study. In addition, the assessment covers a relatively short period immediately after the implementation of the “Go West” program, thus it does not involve the time before baseline. Therefore, future research can include one or more of the followings: 1) incorporating the error from the data processing step to the regression between urban expansion and urban environmental change; 2) monitoring the urban expansion through not only the horizontal but also the vertical direction; 3) exploring the underlying mechanism between urban expansion and urban environment; 4) studying urban expansion and sustainability with a longer time series covering periods before the year of 2000.

CHAPTER 6: CONCLUSIONS

The world is becoming more urbanized than ever with rapid population growth and economic development, which also leads to many undesirable consequences. As one of the most important factors of urban life, residents' living environment is facing challenges from rapid urban expansion. To achieve sustainable urban development, it is imperative to comprehensively assess the urban environment. The present research makes efforts to track the process of urban expansion and evaluate urban environment using the case from Chengdu during 2000-2015 under the background of China's Western Development program. Major contributions are as follows.

The use and advancement of theories, frameworks, methods and techniques enable a comprehensive pixel-base spatial analysis on the urban environment, which gives an example of urban environment evaluation that is applicable to all the cities around the world. First of all, the use of remote sensing and GIS is an efficient and effective way to track the spatial and temporal patterns of urban expansion with high accuracy and high resolution. Second, the integration of self, neighborhood and accessibility dimensions on the urban environment provides a comprehensive assessment. Third, the application of the catastrophe model gives an exemplar of urban environmental assessment that is applicable to almost all indicator-based analysis systems. Fourth, the pixel-based analysis enables the understanding of spatial heterogeneity within administrative boundaries, and this advanced the lump-sum assessments in most of the previous studies, which only give one score for one city.

The results illustrate the relative spatial and temporal changes of urban expansion and the environment. Based on the discussion, the changes of urban expansion and the urban environment are influenced by activities of governments, organizations and companies, while constrained by the existing built environment and geographic condition. The analysis on the relationship between urban expansion and the urban environment supports the view that rapid urban expansion may have negative consequences on the urban environment, but this phenomenon can be alleviated through policy intervention. However, more rigorous analyses need to be done before reaching this conclusion. Using this study as a reference, policy-makers can help future urban planning and sustainable urban development of Chengdu.

REFERENCES

REFERENCES

Artis, D. A., & Carnahan, W. H. (1982). Survey of emissivity variability in thermography of urban areas. Remote Sensing of Environment, 12(4), 313-329.

Antrop, M. (2000). Changing patterns in the urbanized countryside of Western Europe. Landscape ecology, 15(3), 257-270.

Antrop, M. (2004). Landscape change and the urbanization process in Europe. Landscape and urban planning, 67(1-4), 9-26.

Bannari, A., Morin, D., Bonn, F., & Huete, A. R. (1995). A review of vegetation indices. Remote sensing reviews, 13(1-2), 95-120.

Bengston, D. N., Potts, R. S., Fan, D. P., & Goetz, E. G. (2005). An analysis of the public discourse about urban sprawl in the United States: Monitoring concern about a major threat to forests. Forest Policy and Economics, 7(5), 745-756.

Bain, I. (2010). Sustainable development in Western China: managing people, livestock and grasslands in pastoral areas. Mountain Research and Development, 30(1), 59-61.

Batty, M. (2011). When all the world's a city. Environment and Planning A, 43(4), 765-772.

Belgiu, M., & Drăguţ, L. (2016). Random forest in remote sensing: A review of applications and future directions. ISPRS Journal of Photogrammetry and Remote Sensing, 114, 24-31.

Clarke, M., & Wilson, A. G. (1983). The dynamics of urban spatial structure: progress and problems. Journal of regional science, 23(1), 1-18.

Carlson, R. E., & Fritsch, F. N. (1985). Monotone piecewise bicubic interpolation. SIAM journal on numerical analysis, 22(2), 386-400.

Congalton, R. G. (1991). A review of assessing the accuracy of classifications of remotely sensed data. Remote sensing of environment, 37(1), 35-46.

Courdier, R., Guerrin, F., Andriamasinoro, F. H., & Paillat, J. M. (2002). Agent-based simulation of complex systems: application to collective management of animal wastes. Journal of Artificial Societies and Social Simulation, 5(3).

Cheng, J., & Masser, I. (2003). Urban growth pattern modeling: a case study of Wuhan city, PR China. Landscape and urban planning, 62(4), 199-217.

Chen, X. L., Zhao, H. M., Li, P. X., & Yin, Z. Y. (2006). Remote sensing image-based analysis of the relationship between urban heat island and land use/cover changes. Remote Sensing of Environment, 104(2), 133-146.

Colabianchi, N., Dowda, M., Pfeiffer, K. A., Porter, D. E., Almeida, M. J. C., & Pate, R. R. (2007). Towards an understanding of salient neighborhood boundaries: adolescent reports of an easy walking distance and convenient driving distance. International journal of behavioral nutrition and physical activity, 4(1), 66.

Chen, A., & Gao, J. (2011). Urbanization in China and the coordinated development model—The case of Chengdu. The Social Science Journal, 48(3), 500-513.

Chen, Y., & Xie, S. D. (2014). Characteristics and formation mechanism of a heavy air pollution episode caused by biomass burning in Chengdu, Southwest China. Science of the Total Environment, 473, 507-517.

Congalton, R., Gu, J., Yadav, K., Thenkabail, P., & Ozdogan, M. (2014). Global land cover mapping: A review and uncertainty analysis. Remote Sensing, 6(12), 12070-12093.

Deng, X., Huang, J., Rozelle, S., & Uchida, E. (2008). Growth, population and industrialization, and urban land expansion of China. Journal of Urban Economics, 63(1), 96-115.

Dye, C. (2008). Health and urban living. Science, 319(5864), 766-769.

Fensholt, R., Rasmussen, K., Nielsen, T. T., & Mbow, C. (2009). Evaluation of earth observation based long term vegetation trends—Intercomparing NDVI time series trend analysis consistency of Sahel from AVHRR GIMMS, Terra MODIS and SPOT VGT data. Remote Sensing of Environment, 113(9), 1886-1898.

Fox, M. S. (2013). A foundation ontology for global city indicators. University of Toronto, Toronto, Global Cities Institute.

Frumkin, H. (2016). Urban sprawl and public health. Public Health Reports.

FAO. (2017). The future of food and agriculture – Trends and challenges. Rome.

Fan, P., Ouyang, Z., Nguyen, D. D., Nguyen, T. T. H., Park, H., & Chen, J. (2019). Urbanization, economic development, environmental and social changes in transitional economies: Vietnam after Doimoi. Landscape and urban planning, 187, 145-155.

Giridharan, R., Ganesan, S., & Lau, S. S. Y. (2004). Daytime urban heat island effect in high-rise and high-density residential developments in Hong Kong. Energy and buildings, 36(6), 525-534.

Gibson, R. B. (2006). Beyond the pillars: sustainability assessment as a framework for effective integration of social, economic and ecological considerations in significant decision-making. Journal of Environmental Assessment Policy and Management, 8(03), 259-280.

Gao, J., Wei, Y. D., Chen, W., & Chen, J. (2014). Economic transition and urban land expansion in Provincial China. Habitat International, 44, 461-473.

Gascon, M., Triguero-Mas, M., Martínez, D., Dadvand, P., Forns, J., Plasència, A., & Nieuwenhuijsen, M. (2015). Mental health benefits of long-term exposure to residential green and blue spaces: a systematic review. International journal of environmental research and public health, 12(4), 4354-4379.

Gorelick, N., Hancher, M., Dixon, M., Ilyushchenko, S., Thau, D., & Moore, R. (2017). Google Earth Engine: Planetary-scale geospatial analysis for everyone. Remote Sensing of Environment, 202, 18-27.

Hartig, T., Mang, M., & Evans, G. W. (1991). Restorative effects of natural environment experiences. Environment and behavior, 23(1), 3-26.

He, K., Yang, F., Ma, Y., Zhang, Q., Yao, X., Chan, C. K., ... & Mulawa, P. (2001). The characteristics of PM2. 5 in Beijing, China. Atmospheric Environment, 35(29), 4959-4970.

Henderson, M., Yeh, E. T., Gong, P., Elvidge, C., & Baugh, K. (2003). Validation of urban boundaries derived from global night-time satellite imagery. International Journal of Remote Sensing, 24(3), 595-609.

Hengsdijk, H., & Van Ittersum, M. K. (2003). Formalizing agro-ecological engineering for future-oriented land use studies. European Journal of Agronomy, 19(4), 549-562.

He, C., Okada, N., Zhang, Q., Shi, P., & Zhang, J. (2006). Modeling urban expansion scenarios by coupling cellular automata model and system dynamic model in Beijing, China. Applied Geography, 26(3-4), 323-345.

Henríquez, C., Azócar, G., & Romero, H. (2006). Monitoring and modeling the urban growth of two mid-sized Chilean cities. Habitat International, 30(4), 945-964.

Han, L., Zhou, W., Li, W., & Li, L. (2014). Impact of urbanization level on urban air quality: A case of fine particles (PM2. 5) in Chinese cities. Environmental Pollution, 194, 163-170.

He, C., Huang, Z., & Ye, X. (2014). Spatial heterogeneity of economic development and industrial pollution in urban China. Stochastic environmental research and risk assessment, 28(4), 767-781.

He, C., Liu, Z., Tian, J., & Ma, Q. (2014). Urban expansion dynamics and natural habitat loss in China: a multiscale landscape perspective. Global change biology, 20(9), 2886-2902.

Hou, Z., Yang, F., Chen, L., Yang, J., & Yao, Z. (2016). Research About Emigration Behavior of Family in Chengdu Under China's New Urbanization Strategy (No. 16-3125).

Huang, L., Yan, L., & Wu, J. (2016). Assessing urban sustainability of Chinese megacities: 35 years after the economic reform and open-door policy. Landscape and Urban Planning, 145, 57-70.

Jiménez-Muñoz, J. C., Cristóbal, J., Sobrino, J. A., Sòria, G., Ninyerola, M., & Pons, X. (2009). Revision of the single-channel algorithm for land surface temperature retrieval from Landsat thermal-infrared data. IEEE Transactions on geoscience and remote sensing, 47(1), 339-349.

Krämer, U., Koch, T., Ranft, U., Ring, J., & Behrendt, H. (2000). Traffic-related air pollution is associated with atopy in children living in urban areas. Epidemiology, 11(1), 64-70.

Kawabata, A., Ichii, K., & Yamaguchi, Y. (2001). Global monitoring of interannual changes in vegetation activities using NDVI and its relationships to temperature and precipitation. International journal of remote sensing, 22(7), 1377-1382.

Krajnc, D., & Glavič, P. (2005). A model for integrated assessment of sustainable development. Resources, Conservation and Recycling, 43(2), 189-208.

Krausmann, F., Gingrich, S., Eisenmenger, N., Erb, K. H., Haberl, H., & Fischer-Kowalski, M. (2009). Growth in global materials use, GDP and population during the 20th century. Ecological Economics, 68(10), 2696-2705.

Kondo, M., Fluehr, J., McKeon, T., & Branas, C. (2018). Urban green space and its impact on human health. International journal of environmental research and public health, 15(3), 445.

Lai, H. H. (2002). China’s western development program: Its rationale, implementation, and prospects. Modern China, 28(4), 432-466.

Lundin, M., & Morrison, G. M. (2002). A life cycle assessment based procedure for development of environmental sustainability indicators for urban water systems. Urban water, 4(2), 145-152.

Liu, J., Zhan, J., & Deng, X. (2005). Spatio-temporal patterns and driving forces of urban land expansion in China during the economic reform era. AMBIO: a journal of the human environment, 34(6), 450-456.

Lunetta, R. S., Knight, J. F., Ediriwickrema, J., Lyon, J. G., & Worthy, L. D. (2006). Land-cover change detection using multi-temporal MODIS NDVI data. Remote sensing of environment, 105(2), 142-154.

Li, J. J., Wang, X. R., Wang, X. J., Ma, W. C., & Zhang, H. (2009). Remote sensing evaluation of urban heat island and its spatial pattern of the Shanghai metropolitan area, China. *Ecological Complexity*, *6*(4), 413-420.

Li, F., Liu, X., Hu, D., Wang, R., Yang, W., Li, D., & Zhao, D. (2009). Measurement indicators and an evaluation approach for assessing urban sustainable development: A case study for China's Jining City. Landscape and urban planning, 90(3-4), 134-142.

Li, T., Zhang, H., Yuan, C., Liu, Z., & Fan, C. (2012). A PCA-based method for construction of composite sustainability indicators. The International Journal of Life Cycle Assessment, 17(5), 593-603.

Liu, J., & Jin, X. (2012). Study of large-scale planning strategies of new districts under the national policy—A case from Tianfu District in Chengdu, Sichuan (in Chinese). Diversity and tolerance, 2012 collection of China city planning theses.

Li, X., Zhou, W., & Ouyang, Z. (2013). Forty years of urban expansion in Beijing: what is the relative importance of physical, socioeconomic, and neighborhood factors? Applied Geography, 38, 1-10.

Long, H. (2014). Land use policy in China: Introduction. Land Use Policy, 40, 1-5.

Legates, R., & Hudalah, D. (2014). Peri-urban planning for developing East Asia: learning from chengdu, China and Yogyakarta/Kartamantul, Indonesia. Journal of Urban Affairs, 36(sup1), 334-353.

Lillesand, T., Kiefer, R. W., & Chipman, J. (2014). Remote sensing and image interpretation. John Wiley & Sons.

Li, X., Elvidge, C., Zhou, Y., Cao, C., & Warner, T. (2017). Remote sensing of night-time light. International Journal of Remote Sensing, 38(21), 5855-5859.

Liu, J., Hull, V., Godfray, H. C. J., Tilman, D., Gleick, P., Hoff, H., ... & Li, S. (2018). Nexus approaches to global sustainable development. Nature Sustainability, 1(9), 466.

McGahan, P. (1972). The neighbor role and neighboring in a highly urban area. Sociological Quarterly, 13(3), 397-408.

May, R., Rex, K., Bellini, L., Sadullah, S., Nishi, E., James, F., & Mathangani, A. (2000). UN Habitat Indicators Database: evaluation as a source of the status of urban development problems and programs. Cities, 17(3), 237-244.

Maddison, A., (2001). The world economy. A Millenial Perspective. OECD, Paris.

Metzger, M. J., & Schröter, D. (2006). Towards a spatially explicit and quantitative vulnerability assessment of environmental change in Europe. Regional Environmental Change, 6(4), 201-216.

Mitchell, R., & Popham, F. (2008). Effect of exposure to natural environment on health inequalities: an observational population study. The Lancet, 372(9650), 1655-1660.

Moussiopoulos, N., Achillas, C., Vlachokostas, C., Spyridi, D., & Nikolaou, K. (2010). Environmental, social and economic information management for the evaluation of sustainability in urban areas: A system of indicators for Thessaloniki, Greece. Cities, 27(5), 377-384.

Malekmohammadi, B., & Jahanishakib, F. (2017). Vulnerability assessment of wetland landscape ecosystem services using driver-pressure-state-impact-response (DPSIR) model. Ecological Indicators, 82, 293-303.

Nwaka, G. I. (2005). The urban informal sector in Nigeria: towards economic development, environmental health, and social harmony. Global Urban Development Magazine, 1(1), 1-11.

Nuissl, H., Haase, D., Lanzendorf, M., & Wittmer, H. (2009). Environmental impact assessment of urban land use transitions—A context-sensitive approach. Land use policy, 26(2), 414-424.

Neri, A. C., Dupin, P., & Sánchez, L. E. (2016). A pressure–state–response approach to cumulative impact assessment. Journal of cleaner production, 126, 288-298.

Nutsford, D., Pearson, A. L., Kingham, S., & Reitsma, F. (2016). Residential exposure to visible blue space (but not green space) associated with lower psychological distress in a capital city. Health & place, 39, 70-78.

Ouyang, Z., Fan, P., & Chen, J. (2016). Urban built-up areas in transitional economies of Southeast Asia: Spatial extent and dynamics. Remote Sensing, 8(10), 819.

Pacione, M. (2003). Urban environmental quality and human wellbeing—a social geographical perspective. Landscape and urban planning, 65(1-2), 19-30.

Pettorelli, N., Vik, J. O., Mysterud, A., Gaillard, J. M., Tucker, C. J., & Stenseth, N. C. (2005). Using the satellite-derived NDVI to assess ecological responses to environmental change. Trends in ecology & evolution, 20(9), 503-510.

Pui, D. Y., Chen, S. C., & Zuo, Z. (2014). PM2. 5 in China: Measurements, sources, visibility and health effects, and mitigation. Particuology, 13, 1-26.

Peng, W., Wang, G., Zhou, J., Zhao, J., & Yang, C. (2015). Studies on the temporal and spatial variations of urban expansion in Chengdu, western China, from 1978 to 2010. Sustainable Cities and Society, 17, 141-150.

Qin, Z., Karnieli, A., & Berliner, P. (2001). A mono-window algorithm for retrieving land surface temperature from Landsat TM data and its application to the Israel-Egypt border region. International journal of remote sensing, 22(18), 3719-3746.

Qiao, X., Jaffe, D., Tang, Y., Bresnahan, M., & Song, J. (2015). Evaluation of air quality in Chengdu, Sichuan Basin, China: are China's air quality standards sufficient yet?. Environmental monitoring and assessment, 187(5), 250.

Rouse, J. W. (1974). Monitoring the vernal advancement of retrogradation of natural vegetation, NASA/GSFG, Type III. Final Report, 371.

Rosenfield, G. H., Fitzpatrick-Lins, K., & Ling, H. S. (1982). Sampling for thematic map accuracy testing. Photogrammetric Engineering and Remote Sensing, 48(1), 131-137.

Root, E. D. (2012). Moving neighborhoods and health research forward: using geographic methods to examine the role of spatial scale in neighborhood effects on health. Annals of the Association of American Geographers, 102(5), 986-995.

Schwirian, K. P., & Prehn, J. W. (1962). An axiomatic theory of urbanization. American Sociological Review, 812-825.

Stehman, S. V. (1997). Selecting and interpreting measures of thematic classification accuracy. Remote sensing of Environment, 62(1), 77-89.

Shibata, T., Solo-Gabriele, H. M., Fleming, L. E., & Elmir, S. (2004). Monitoring marine recreational water quality using multiple microbial indicators in an urban tropical environment. Water research, 38(13), 3119-3131.

Schneider, A., Seto, K. C., & Webster, D. R. (2005). Urban growth in Chengdu, Western China: application of remote sensing to assess planning and policy outcomes. Environment and Planning B: Planning and Design, 32(3), 323-345.

Schneider, A., & Woodcock, C. E. (2008). Compact, dispersed, fragmented, extensive? A comparison of urban growth in twenty-five global cities using remotely sensed data, pattern metrics and census information. Urban Studies, 45(3), 659-692.

Seto, K. C., & Satterthwaite, D. (2010). Interactions between urbanization and global environmental change. Current Opinion in Environmental Sustainability, 3(2), 127-128.

Seto, K. C., Fragkias, M., Güneralp, B., & Reilly, M. K. (2011). A meta-analysis of global urban land expansion. PloS ONE, 6(8), e23777.

Shen, L. Y., Ochoa, J. J., Shah, M. N., & Zhang, X. (2011). The application of urban sustainability indicators–A comparison between various practices. Habitat international, 35(1), 17-29.

Su, S., Li, D., Yu, X., Zhang, Z., Zhang, Q., Xiao, R., Zhi, J., & Wu, J. (2011). Assessing land ecological security in Shanghai (China) based on catastrophe theory. Stochastic Environmental Research and Risk Assessment, 25(6), 737-746.

Schneider, A. (2012). Monitoring land cover change in urban and peri-urban areas using dense time stacks of Landsat satellite data and a data mining approach. Remote Sensing of Environment, 124, 689-704.

Shao, H., Sun, X., Tao, S., Xiang, Z., & Xian, W. (2015). Environmental vulnerability assessment in middle-upper reaches of Dadu River Watershed using Projection Pursuit Model and GIS. Carpathian Journal of Earth and Environmental Sciences, 10(4), 133-146.

Simon, D., Arfvidsson, H., Anand, G., Bazaz, A., Fenna, G., Foster, K., ... & Nyambuga, C. (2016). Developing and testing the Urban Sustainable Development Goal’s targets and indicators–a five-city study. Environment and Urbanization, 28(1), 49-63.

Shen, H., Huang, L., Zhang, L., Wu, P., & Zeng, C. (2016). Long-term and fine-scale satellite monitoring of the urban heat island effect by the fusion of multi-temporal and multi-sensor remote sensed data: A 26-year case study of the city of Wuhan in China. Remote Sensing of Environment, 172, 109-125.

Tran, H., Uchihama, D., Ochi, S., & Yasuoka, Y. (2006). Assessment with satellite data of the urban heat island effects in Asian mega cities. International journal of applied Earth observation and Geoinformation, 8(1), 34-48.

Taubenböck, H., Esch, T., Felbier, A., Wiesner, M., Roth, A., & Dech, S. (2012). Monitoring urbanization in mega cities from space. Remote sensing of Environment, 117, 162-176.

Tao, J., Zhang, L., Engling, G., Zhang, R., Yang, Y., Cao, J., ... & Luo, L. (2013). Chemical composition of PM2. 5 in an urban environment in Chengdu, China: Importance of springtime dust storms and biomass burning. Atmospheric Research, 122, 270-283.

Unger, D. G., & Wandersman, A. (1982). Neighboring in an urban environment. American Journal of Community Psychology, 10(5), 493-509.

United Nations (2011). National Accounts Main Aggregates Database. United Nations Statistics Division, New York.

United Nations (2014). World Urbanization Prospects: The 2014 Version-Highlights. Department of Economic and Social Affairs. New York.

Ulmer, J. M., Wolf, K. L., Backman, D. R., Tretheway, R. L., Blain, C. J., O'Neil-Dunne, J. P., & Frank, L. D. (2016). Multiple health benefits of urban tree canopy: The mounting evidence for a green prescription. Health & Place, 42, 54-62.

Van de Griend, A., & Owe, M. (1993). On the relationship between thermal emissivity and the normalized difference vegetation index for natural surfaces. International Journal of Remote Sensing, 14, 1119–1131.

Valor, E., & Caselles, V. (1996). Mapping land surface emissivity from NDVI: Application to European, African, and South American areas. Remote sensing of Environment, 57(3), 167-184.

Voth, H. J. (2004). Living standards and the urban environment. The Cambridge Economic History of Modern Britain, 1, 1700-1860.

Van de Kerk, G., & Manuel, A. R. (2008). A comprehensive index for a sustainable society: The SSI—the Sustainable Society Index. Ecological Economics, 66(2-3), 228-242.

Van Donkelaar, A., Martin, R. V., Brauer, M., Hsu, N. C., Kahn, R. A., Levy, R. C., ... & Winker, D. M. (2016). Global estimates of fine particulate matter using a combined geophysical-statistical method with information from satellites, models, and monitors. Environmental science & technology, 50(7), 3762-3772.

Woodstock, A. E. R., & Poston, T. (2006). A geometrical study of the elementary catastrophes (Vol. 373). Springer.

Woodcock, C. E., Allen, R., Anderson, M., Belward, A., Bindschadler, R., Cohen, W., ... & Nemani, R. (2008). Free access to Landsat imagery. Science, 320(5879), 1011-1011.

Walcott, S. M. (2007). The dragon's tail: Utilizing Chengdu and Chongqing technology development zones to anchor west China economic advancement. Journal of Chinese Economic and Business Studies, 5(2), 131-145.

Wulder, M. A., White, J. C., Goward, S. N., Masek, J. G., Irons, J. R., Herold, M., ... & Woodcock, C. E. (2008). Landsat continuity: Issues and opportunities for land cover monitoring. Remote Sensing of Environment, 112(3), 955-969.

Weinmayr, G., Romeo, E., De Sario, M., Weiland, S. K., & Forastiere, F. (2009). Short-term effects of PM10 and NO2 on respiratory health among children with asthma or asthma-like symptoms: a systematic review and meta-analysis. Environmental health perspectives, 118(4), 449-457.

Wilson, A. (2011). Catastrophe theory and bifurcation: applications to urban and regional systems. Routledge.

Wang, H., He, Q., Liu, X., Zhuang, Y., & Hong, S. (2012). Global urbanization research from 1991 to 2009: A systematic research review. Landscape and urban planning, 104(3-4), 299-309.

Wei, Y. D., & Ye, X. (2014). Urbanization, urban land expansion and environmental change in China. Stochastic environmental research and risk assessment, 28(4), 757-765.

Wu, J., Xiang, W. N., & Zhao, J. (2014). Urban ecology in China: Historical developments and future directions. Landscape and Urban Planning, 125, 222-233.

Wei, Y. D., Li, H., & Yue, W. (2017). Urban land expansion and regional inequality in transitional China. Landscape and Urban Planning, 163, 17-31.

Weiss, D. J., Nelson, A., Gibson, H. S., Temperley, W., Peedell, S., Lieber, A., ... & Mappin, B. (2018). A global map of travel time to cities to assess inequalities in accessibility in 2015. Nature, 553(7688), 333.

Xu, H. X., Dan, S. M., & He, Z. W. (2007). Remote sensing analysis of urban heat island effect in Chengdu Plain (in Chinese). Environmental Science & Technology, 8, 21-23.

Xie, Q., Zhou, Z., Teng, M., & Wang, P. (2012). A multi-temporal Landsat TM data analysis of the impact of land use and land cover changes on the urban heat island effect. Journal of Food, Agriculture & Environment, 10(2 part 2), 803-809.

Yagoub, M. M. (2004). Monitoring of urban growth of a desert city through remote sensing: Al-Ain, UAE, between 1976 and 2000. International Journal of Remote Sensing, 25(6), 1063-1076.

Yang, F., Shao, D., Xiao, C., & Tan, X. (2012). Assessment of urban water security based on catastrophe theory. Water science and technology, 66(3), 487-493.

Yue, W., Liu, Y., Fan, P., Ye, X., & Wu, C. (2012). Assessing spatial pattern of urban thermal environment in Shanghai, China. Stochastic environmental research and risk assessment, 26(7), 899-911.

Ye, Y., LeGates, R., & Qin, B. (2013). Coordinated urban-rural development planning in China: the Chengdu model. Journal of the American Planning Association, 79(2), 125-137.

Yue, W., Fan, P., Wei, Y. D., & Qi, J. (2014). Economic development, urban expansion, and sustainable development in Shanghai. Stochastic environmental research and risk assessment, 28(4), 783-799.

Yu, X., Guo, X., & Wu, Z. (2014). Land surface temperature retrieval from Landsat 8 TIRS—Comparison between radiative transfer equation-based method, split window algorithm and single channel method. Remote Sensing, 6(10), 9829-9852.

Yigitcanlar, T., Dur, F., & Dizdaroglu, D. (2015). Towards prosperous sustainable cities: A multiscalar urban sustainability assessment approach. Habitat International, 45, 36-46.

Zha, Y., Gao, J., & Ni, S. (2003). Use of normalized difference built-up index in automatically mapping urban areas from TM imagery. International journal of remote sensing, 24(3), 583-594.

Zhao, S., Da, L., Tang, Z., Fang, H., Song, K., & Fang, J. (2006). Ecological consequences of rapid urban expansion: Shanghai, China. Frontiers in Ecology and the Environment, 4(7), 341-346.

Zhu, Z., & Woodcock, C. E. (2014). Continuous change detection and classification of land cover using all available Landsat data. Remote sensing of Environment, 144, 152-171.

Zhou, D., Zhao, S., Liu, S., Zhang, L., & Zhu, C. (2014). Surface urban heat island in China's 32 major cities: Spatial patterns and drivers. Remote Sensing of Environment, 152, 51-61.

Zhao, W., & Yang, J. (2016). Rural Planning in the New Urbanization Process: The Case of Chengdu, China. In Urbanization and Locality (pp. 111-120). Springer, Berlin, Heidelberg.

Zhang, Q., Song, C., & Chen, X. (2018). Effects of China’s payment for ecosystem services programs on cropland abandonment: A case study in Tiantangzhai Township, Anhui, China. Land Use Policy, 73, 239-248.

Zhou, W., Ma, T., Chen, L., Wu, L., & Luo, Y. (2018). Application of catastrophe theory in comprehensive ecological security assessment of plastic greenhouse soil contaminated by phthalate esters. PloS one, 13(10), e0205680.